2022

Modeling Pa-233 Generation in Thorium-Fueled Reactors for Safeguards

Victoria Davis
Virginia Commonwealth University

MODELING ^{233}PA GENERATION IN THORIUM-FUELED REACTORS FOR SAFEGUARDS

by

VICTORIA DAVIS

A Thesis Submitted to the Graduate School of

VIRGINIA COMMONWEALTH UNIVERSITY

In Partial Fulfillment of the Requirements for the Degree

MASTER OF SCIENCE

in

MECHANICAL AND NUCLEAR ENGINEERING

MAY 2022

Approved

Braden Goddard, Advisor

Supathorn Phongikaroon

George W. Hitt

ACKNOWLEDGEMENTS

The author would like to thank the NNSA's Office of International Nuclear Safeguards (NA-241) for supporting this work.

TABLE OF CONTENTS

LIST OF FIGURES

LIST OF ABBREVIATIONS

AWCC	Active Well Coincidence Counter
CANDU	Canada Deuterium Uranium reactor
DA	Destructive Assay
GWd/MTHM	Gigawatt-Days per Metric Ton of Heavy Metal
HKED	Hybrid K-Edge Densitometry
HPGe	High-Purity Germanium detector
IAEA	International Atomic Energy Agency
ICP-MS	Inductively Coupled Plasma Mass Spectrometry
KED	K-Edge Densitometry
LA-MC-ICP-MS	Laser Ablation Multi-Collector Inductively Coupled Mass Spectrometry
LIBS	Laser-Induced Breakdown Spectroscopy
MCNP	Monte Carlo N-Particle
MSR	Molten Salt Reactor
NaI	Sodium Iodide detector
NDA	Non-Destructive Assay
ORIGEN	Oak Ridge Isotope Generation

PHWR	Pressurized Heavy Water Reactor
PWR	Pressurized Water Reactor
SBD	Safeguards-by-design
SCALE	Standardized Computer Analyses for Licensing Evaluation
SD-TMSR	Single-fluid Double-zoned Thorium Molten Salt Reactor
TIMS	Thermal Ionization Mass Spectrometry
TRITON	Transport Rigor Implemented with Time-dependent Operation for Neutronic depletion
XRF	X-ray Fluorescence

ABSTRACT

Thorium has been researched for many decades as a possible alternative to uranium nuclear fuel. Thorium can be implemented in many different reactor designs including pressurized water reactors (PWRs), pressurized heavy water reactors (PHWRs), and molten salt reactors (MSRs). Its abundance in the earth, decreased long-lived transuranic waste, and claims that there are fewer proliferation concerns contribute to the attractiveness of using thorium as alternative nuclear fuel. However, possible proliferation pathways have been noted and must be investigated, particularly the potential diversion of ^{233}Pa which can then decay to ^{233}U – special fissionable material that should be under International Atomic Energy Agency (IAEA) safeguards.

To better understand the concern of this potential proliferation challenge of thorium, different nuclear material accountancy techniques were reviewed for their viability to quantify ^{233}Pa if extracted from irradiated thorium fuel. Quantifying and tracking ^{233}Pa is important for safeguards because ^{233}Pa is a precursor for ^{233}U. Without monitoring ^{233}Pa, it is possible to produce high purity ^{233}U outside of the safeguards monitoring system. Characteristics of interest of different material accountancy techniques included technology maturity, cost, precision, and time taken to acquire results. Some technologies, like hybrid K-edge densitometry (HKED) and passive gamma spectroscopy, appear to be viable techniques based on current literature. Due to the limited scope of this project, only passive gamma spectroscopy was further investigated.

Three different reactor types (PWR, CANDU, MSR) were modeled with mixed thorium-uranium oxide fuels that were burned until the fuel was spent. The protactinium in the used fuel was extracted at the time of shutdown and the change in isotopic content of the protactinium quantified. Gamma spectroscopy simulations were performed for the protactinium isotopes and their decay products at various decay times to understand protactinium generation within the

reactor cores. Given the simplicity of the models and large assumptions made (e.g. no background, no shielding, no self-attenuation), the initial results indicate that though ^{233}Pa is detectable for each reactor fuel types modeled at all decay times (0 to 300 days), more work should be completed with higher fidelity models.

1. INTRODUCTION

1.1. Motivation

As nuclear energy evolves, it is necessary to consider how these changes will affect the measures that must be taken to ensure proper safeguards methods are applied to any new systems or structures. As of December 2020, there were 94 operating nuclear reactors in the United States accounting for 20% of energy generation in the country [1]. Nuclear energy offers a clean and reliable energy source. Using nuclear energy eliminates hundreds of millions of metric tons of carbon emissions per year in the United States alone. It also has the highest capacity factor of any energy source at 92.5%, meaning nuclear power plants are producing 92.5% of their maximum output in a year. This is due to nuclear power plants requiring less shut down time for maintenance and refueling purposes than natural gas and coal, and renewable energy sources often suffer from lack of consistent wind, sun, or water [2].

Uranium and plutonium, both found in nuclear reactors, have fissile isotopes (^{233}U, ^{235}U, ^{239}Pu) that can be used as the fissile core in nuclear weapons. This means that nuclear reactors have the inherent potential to cause proliferation threats. These threats may come from states or non-states trying to obtain unauthorized nuclear material out of a nuclear reactor designed for peaceful purposes. Organizations such as the International Atomic Energy Agency (IAEA) are put in place to ensure the use of nuclear energy for peaceful purposes by monitoring nuclear facilities. The IAEA must constantly adapt to new nuclear technology and understand how to best safeguard against proliferation concerns.

Thorium has been considered a possible alternative to uranium for nuclear fuel for many decades. It is three to four times more abundant in the earth than uranium and produces

significantly less long-lived transuranic nuclear waste. Some claims state thorium poses fewer proliferation concerns than other fuel types largely due to ^{232}U buildup (and associated high energy gamma-emitting decay products) in the irradiated thorium fuel [3]. However, to fully explore potential proliferation concerns, generation and subsequent decay of ^{233}Pa produced in these thorium-fueled reactor cores must be studied. With a half-life of 27 days, ^{233}Pa decays to ^{233}U, which is an IAEA-defined special fissionable material that can be used for nuclear weapons production [4]. With more research being dedicated to thorium-fueled reactors, and several of these reactor designs possessing online fuel processing (allowing for on-site protactinium separation), it is important to understand this potential proliferation pathway. In particular, it is theoretically possible to extract unsecured ^{233}Pa from the irradiated fuel salt before it decays into ^{233}U. This hypothetical potential diversion can become an even greater proliferation concern if the extracted protactinium is purified through a second separation of protactinium isotopes approximately ten days later to remove the short half-life decay products of ^{232}Pa and ^{234}Pa. Thus, this would result in a higher concentration of the ^{233}Pa isotope – a direct parent radionuclide of ^{233}U.

Many countries have shown interest in thorium-fueled nuclear reactors, and many different designs have been researched [5]: Canada and China have worked on Canada Deuterium Uranium (CANDU) reactors; India designed an advanced heavy water reactor; Germany, Brazil, Norway, and Russia have all researched pressurized light water reactors; Germany and the United Kingdom have operated high-temperature gas-cooled reactors, and research is ongoing for molten-salt reactors in China, Japan, Russia, France, and the United States. The potential wide-spread use of next-generation thorium-fueled reactors compels the international safeguards community to assess the ramifications of increased global ^{233}U production through its ^{233}Pa parent nuclide.

1.2. Objectives

This research aims to evaluate the potential proliferation concern regarding ^{233}Pa production in thorium-fueled nuclear reactors and provides possible approaches to assuring timely detection of possible ^{233}Pa diversion. To investigate this proliferation pathway, three types of reactors were modeled to simulate the used fuel upon discharge. The protactinium was immediately separated from the used fuel and gamma spectra were produced for this separated protactinium and its decay products for various time steps up to 300 days after discharge. Given the simplicity of the models and large assumptions made (e.g. no background, no shielding, no self-attenuation), the initial results indicate that though ^{233}Pa is detectable for each reactor fuel types modeled at all decay times, more work should be completed with higher fidelity models.

1.3. Background

1.3.1. Introduction to Nuclear Reactors

Nuclear energy is produced through the fission of atoms in a nuclear reactor. Neutrons are used to collide with fissile nuclides – nuclides able to undergo nuclear fission and maintain a chain reaction – and cause them to split and release energy. This fission produces heat that can then be used to convert water into steam. The steam spins turbines that produce electricity through electrical generators.

There are many different types of nuclear reactors. The most common is the pressurized water reactor (PWR), a type of light water reactor whose schematic is shown in Figure 1. Generally, these reactors use enriched uranium (3-5% ^{235}U) oxide fuel formed into small, cylindrical pellets and stacked in fuel rods. The fuel rods are usually made of zircaloy, a zirconium alloy, and are bundled together to create fuel assemblies. PWRs usually have about 150-250 fuel

assemblies, each containing about 200-300 fuel rods. Control rods are also inserted into the fuel assemblies when necessary to absorb neutrons and control the chain reaction. A moderator is used in the reactor to slow down the neutrons and increase their likelihood of interacting with the uranium atoms. Coolant is also present in the reactor with the purpose of removing heat from the core to the electrical generators. The moderator and coolant in PWRs are both light water (^1H_2O). Nuclear reactors need to be refueled periodically to replace the irradiated fuel with fresh fuel. PWRs are typically shut down for refueling every 18 to 24 months, but this refueling process can take weeks. The amount of energy obtained from the fuel is calculated as burnup, or a measure of how much heavy metal has undergone nuclear fission. Average burnup values for PWRs are around 40 to 50 GWd/MTHM (gigawatt-days per metric ton of heavy metal) [6].

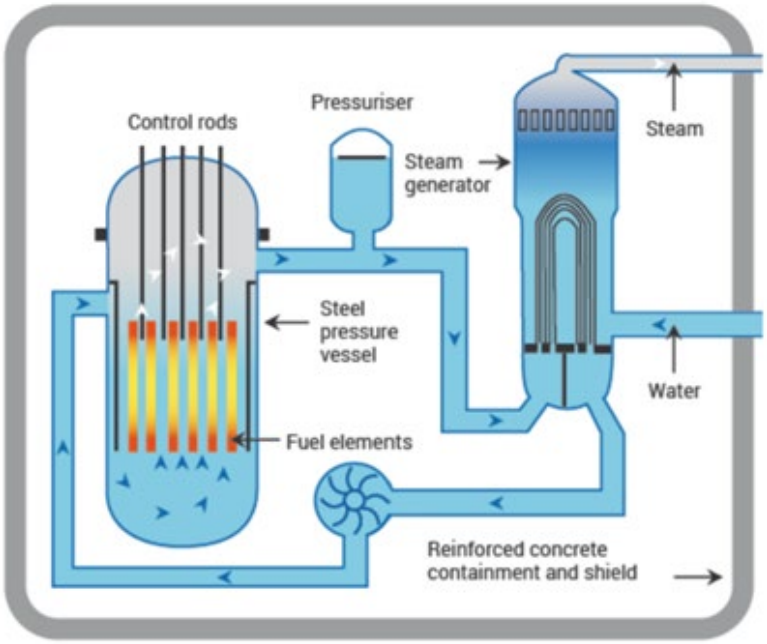

Figure 1: Diagram of a pressurized water reactor (PWR) [7].

Another type of reactor is the pressurized heavy water reactor (PHWR), the most common type being a CANDU reactor (schematic shown in Figure 2). No PHWRs are in commercial use

in the United States, but they can be seen in many countries throughout the world. They function similarly to PWRs, however, they use deuterium oxide, i.e. heavy water (^2H_2O), as the moderator. PHWRs generally use natural uranium (0.711% ^{235}U) for the fuel, although a wide spectrum of different fuel enrichments and compositions have been tested in PHWRs. PHWRs can also perform online refueling, meaning the reactor does not need to be shut down for the refueling process. Since the fuel assemblies are arranged horizontally in a PHWR (unlike the vertical arrangement in PWRs) fuel assemblies can be inserted on one side and removed from the other side of the core [8]. The online refueling is also allowed due to the reactors using a pressure-tube design rather than a pressure-vessel design to contain the high pressure in the reactor. In PWRs, the fuel, coolant, and moderator are contained in a vessel. However, in a PHWR, the moderator is kept separate from the fuel and coolant [9]. These reactors usually only have 28 or 37 fuel rods in an assembly. The burnups generally reach values of 7 to 8 GWd/MTHM.

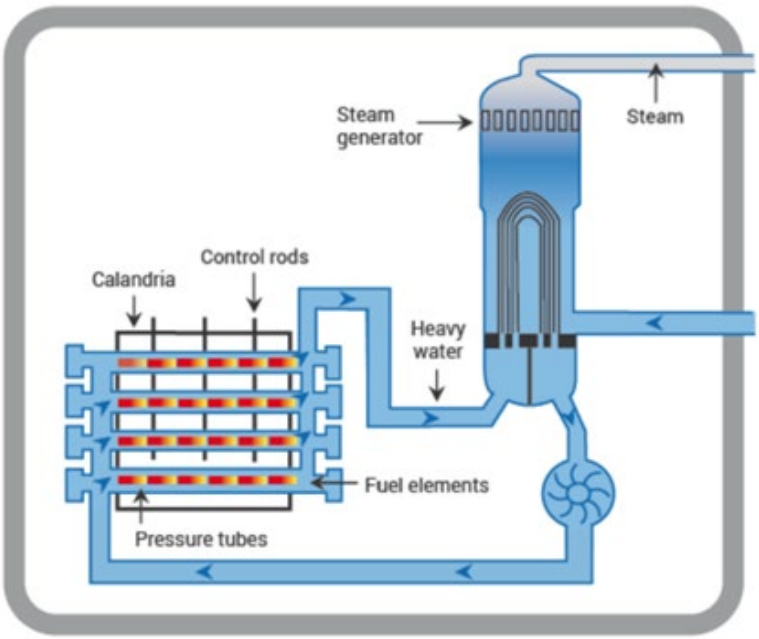

Figure 2: Diagram of a pressurized heavy water reactor (PHWR) [7].

Molten salt reactors (MSRs), with the schematic shown in Figure 3, are another type of reactor that is being heavily researched for possible use with uranium or thorium fuels [5]. Unlike current generation nuclear reactors, MSRs use molten salt as the coolant rather than water. Most MSR concepts also use liquid fuel rather than solid fuel [10]. The fuel is combined with a liquid salt mixture, usually lithium-beryllium fluoride. The fuel itself could be thorium, uranium, or plutonium fluoride. Using molten salt fuel can have many benefits, most notably it allows the reactor to operate with a higher thermal efficiency. MSRs also have improved safety features over other reactors that add to their desirability. Since molten salts have high thermal stability, these reactors can operate at high temperatures while remaining at lower pressure [11]. Another safety feature added to MSRs is that if the fuel overheats, it will melt the freeze plug and the fuel will drain into the holding tank. This action is done due to gravity and therefore does not rely on human intervention. In some MSR designs, graphite is used as a moderator. MSRs can have single-fluid or two-fluid designs. Two-fluid MSRs improve the breeding capabilities of the reactor. This means that the reactor has one fluid as a breeder fluid and one fluid as fuel. The purpose of a breeder fluid is to generate more fissile material in the fuel than the reactor consumes. Thorium is a fertile material, not fissile, therefore thorium-fueled MSRs (and all thorium-fueled reactors), must initially start with some amount of fissile material, such as ^{233}U, ^{235}U, or ^{239}Pu, in order to begin the chain reaction process. Fertile materials cannot maintain a fission chain reaction themselves but can be converted into fissile materials. The breeder for these reactors would have thorium fluoride that would produce ^{233}U that could then be used in the fuel fluid as fissile material. A single-fluid design would simply have one fluid containing the fuel (fertile and fissile nuclides) and coolant [12]. As shown in Figure 3, many MSR designs include online reprocessing of the fuel salt so that some of the irradiated fuel may be removed for a time from the reactor core for

treatment and combined with fresh fuel salt before being returned to the core. The concept of the MSR has been around for many decades, however they are not yet widely used. With more research being invested in MSRs, some anticipate their use in the near future.

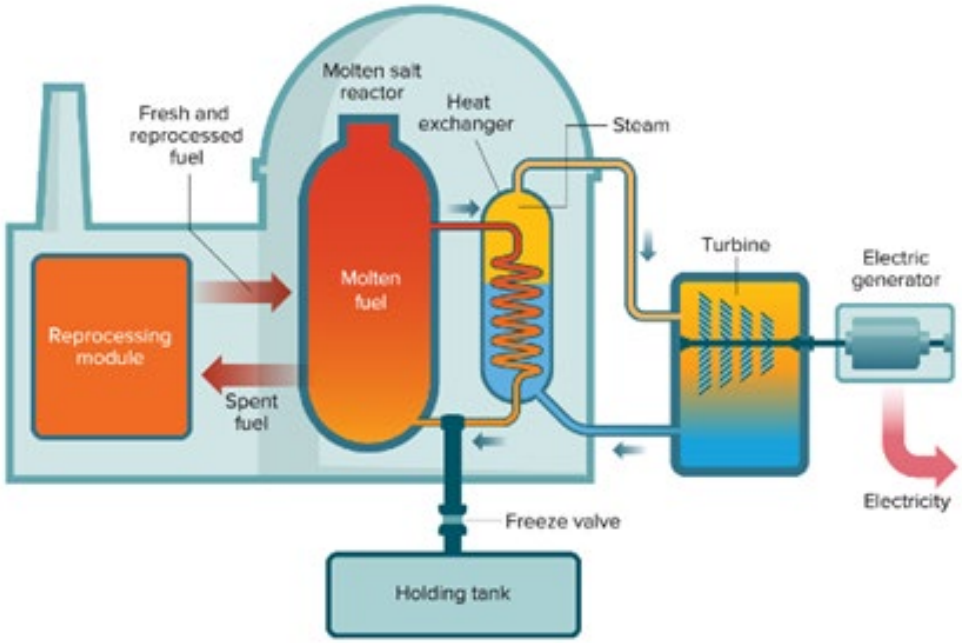

Figure 3: Diagram of a molten salt reactor (MSR) [13].

1.3.2. Introduction to Safeguards

The IAEA was put in place to allow non-weapon states to use nuclear power, while still monitoring their use to deter diversion of nuclear materials for malicious purposes. Safeguards techniques are used to ensure that states are appropriately using their facilities. The IAEA defines safeguards as "the timely detection of diversion of significant quantities of nuclear material from peaceful nuclear activities to the manufacture of nuclear weapons or of other nuclear explosive devices or for purposes unknown, and deterrence of such diversion by the risk of early detection [4]". Three main components of safeguards include material accountability, physical security, and containment and surveillance. Material accountability uses detection methods to verify that a

nuclear facility has all of its nuclear materials accounted for. Physical security would include limiting access to certain areas of the nuclear facility. Containment and surveillance methods use optical and other surveillance methods (both human and instrument observation) and sealing systems with tamper indicating devices [14].

Current safeguards use item accounting or bulk accounting for different steps in the nuclear fuel cycle. Item accounting is used when there are discrete items that can be counted. Bulk accounting is used when materials cannot be counted in discrete form. Nuclear reactors generally used item accounting, but liquid fuels pose a challenge to this and must be treated differently.

The IAEA defines ^{233}U as special fissionable material [15]. Specifically, the IAEA Statute in Article XXI states "the term 'special fissionable material' means plutonium-239; uranium-233; uranium enriched in the isotopes 235 or 233; any material containing one or more of the foregoing; and such other fissionable material as the Board of Governors shall from time to time determine; but the term 'special fissionable material' does not include source material [15]." The IAEA specifies in the IAEA Safeguards Glossary that any quantity of ^{233}U over 8 kg is considered a significant quantity, which is "the approximate amount of nuclear material for which the possibility of manufacturing a nuclear explosive device cannot be excluded [4]". Despite its lack of official designation, if left to decay, diverted ^{233}Pa can produce quantities of ^{233}U that could fall outside of safeguards. If 8 kg of ^{233}Pa is diverted, the significant quantity of 8 kg of ^{233}U could eventually be reached. According to the IAEA Safeguards Glossary, diversion of material is classified as either an abrupt diversion or protracted diversion. This is dependent on the amount of material diverted within the material balance period, or the time between physical inventory takings. If the amount of diverted material is equal to or exceeds one significant quantity in less time than the material balance period, it is considered abrupt diversion. A more gradual diversion

is considered a protracted diversion [4]. Given the decay relationship between ^{233}Pa and ^{233}U, it may be advisable for the IAEA to include it in the list of materials monitored by the IAEA. The issue of the authority to monitor ^{233}Pa is important and must be explored further but is beyond the scope of this project.

1.3.3. Potential Thorium-fueled Reactors Safeguards Challenges

The majority of thorium-based fuel consists of the ^{232}Th isotope. In the reactor, ^{232}Th absorbs a neutron and becomes ^{233}Th. Subsequently, ^{233}Th beta decays (with a half-life of 22 minutes) to ^{233}Pa which, in turn, beta decays with a half-life of 27 days to ^{233}U [3] [16]. The full reaction and decay paths of ^{232}Th are shown in Figure 4. Under the international safeguards regime, ^{233}U falls under IAEA safeguards. In contrast, ^{233}Pa does not. ^{233}Pa is not designated as an alternative nuclear material by the IAEA, which means unmonitored generation of ^{233}Pa can potentially lead to unmonitored diversion of ^{233}U.

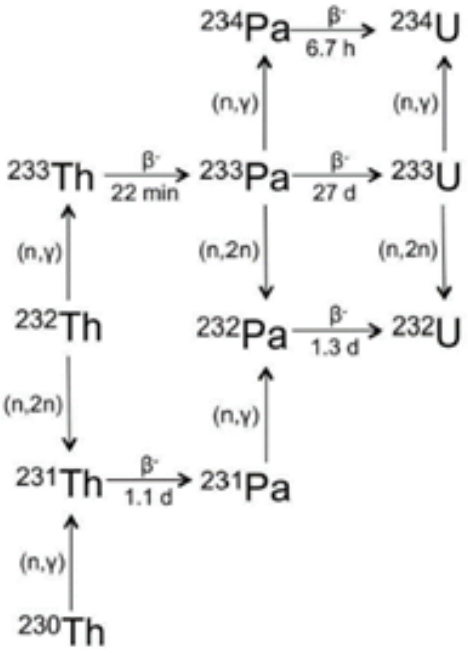

Figure 4: ^{232}Th absorbs a neutron to become ^{233}Th and then beta decays twice to become ^{233}U [16].

It is useful to examine the products of the thorium nuclear fuel cycle to determine if ^{233}Pa could be relatively easily removed from the reactor without detection. This particularly becomes an issue for certain MSR concepts under development. MSRs present new challenges that are not seen in other reactor designs [10]. Many have fuel, coolant, fission products, and actinides mixed in one homogeneous liquid. MSR fuel is not contained in fuel assemblies, and many designs employ an online reprocessing capability in which irradiated fuel salt that has been removed from the reactor core is treated before being returned to the reactor core while the reactor is in operation. Current material accountancy methods are ill-equipped for dealing with the new challenges of the MSR. Since the fuel is liquid, the isotopic concentration will be continuously varying. It would also be considerably difficult to take passive radiation-based measurements due to the fuel being highly radioactive and the reactor operating at very high temperatures (~700ºC). Furthermore, with liquid fissile material, challenges arise in defining appropriate material accountancy approaches regarding item versus bulk accounting facilities or defining strategic measurement points. Regarding MSRs, the IAEA states

> "Designers should be aware that such reactors cannot be considered item facilities… [and] more stringent nuclear material accountancy measures will likely be required to verify the quantities, locations and movements of the nuclear material. These measures can include, but are not limited to, fuel flow monitors, seals, video surveillance, the use of sensors to trigger other sensors, more accurate NDA measurements and sampling plans... Most of this instrumentation does not yet exist and a significant R&D effort can be expected. [17]"

This further emphasizes the fact that current material accountancy methods are not satisfactory for MSRs. Already challenging, using thorium fuel adds complexity to the quantification of nuclear material in an operational MSR. Because of these numerous complications in defining appropriate safeguards approaches for MSRs, many have proposed developing innovative safeguards measures in conjunction with facility designers (i.e., safeguards-by-design or SBD) in the initial stages of MSR development [18]. The IAEA defines SBD as, "the process of including international safeguards considerations throughout all phases of

a nuclear facility life cycle; from the initial conceptual design to facility construction and into operations, including design modifications and decommissioning. Good systems engineering practice requires the inclusion of all relevant requirements early in the design process to optimize the system to perform effectively at the lowest cost and minimum risk [17].” The process of developing safeguards measures via SBD would advance the IAEA and international nuclear safeguards community’s understanding of proper safeguards techniques for MSRs.

In several MSR designs, fuel salt is removed from the reactor core and protactinium is purposefully separated [19]. Removal of protactinium from the core reduces the potential for neutron reactions that will transmute ^{233}Pa to other isotopes of protactinium. As shown in Figure 4, ^{233}Pa can absorb a low-energy (“thermal”) neutron to become ^{234}Pa, which quickly beta decays to become non-fissile ^{234}U; and it can undergo a (n,2n) reaction with a high-energy (“fast”) neutron to become ^{232}Pa, which beta decays to become ^{232}U. Away from the presence of neutron radiation, ^{233}Pa beta decays to ^{233}U [16]. The ^{233}U can then be added back into the reactor core as fissile fuel [20]. This process of removing ^{233}Pa and returning to the reactor after it decays to ^{233}U improves fuel utilization and is vital for thorium fueled breeder reactors. When protactinium is separated from the fuel salt, it inevitably includes some ^{232}Pa and ^{234}Pa. After 10 days there would be a large decrease of ^{232}Pa ($T_{½}$ = 1.32 days) and ^{234}Pa ($T_{½}$ = 0.279 days) present due to their relatively short half-lives, leaving ^{233}Pa ($T_{½}$ = 27.0 days) to make up a larger fraction of the protactinium isotopes in the mixture. At this time, a second separation of protactinium from the uranium and other decay products can be performed, and the separated protactinium can be left to decay again, where its high ^{233}Pa content eventually yields a high purity of ^{233}U. Figure 5 shows that after 10 days (240 hours) there are relatively minuscule amounts of ^{232}Pa and ^{234}Pa left. This could increase the proliferation concern of reactors whose fuel can be reprocessed shortly after leaving the reactor. The presence of ^{232}U may offer some defense against diversion and weaponization due to decay

products (such as ^{208}Tl) that emit high energy gamma rays [20]. These high energy gamma ray emitting decay products would require more safety measures to handle the material but would also make the material detectable and add other challenges for potential proliferation diversion [21] [22].

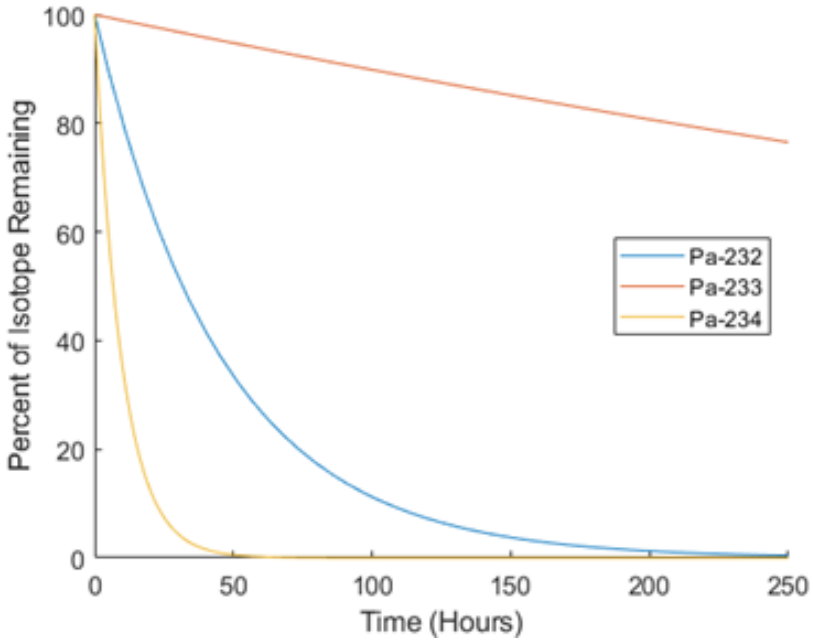

Figure 5: Decay of ^{232}Pa, ^{233}Pa, and ^{234}Pa after being separated from the thorium fuel.

1.3.4. Evaluation of Nuclear Material Accountancy Techniques

Under IAEA safeguards many material accountancy techniques consisting of destructive assay (DA) and non-destructive assay (NDA) technologies, are used to account for nuclear materials in facilities. In the following section, material measurement techniques for the detection of ^{233}Pa were identified and their assay capabilities evaluated to identify a viable and practical technique. Many factors were important in this evaluation, including technology maturity, cost, precision, and duration to acquire results.

Destructive Assay (DA) Techniques

According to the IAEA Safeguards Glossary, destructive assay is the "determination of nuclear material content and, if required, of the isotopic composition of chemical elements present in the sample. Destructive analysis normally involves destruction of the physical form of the sample [4]." In both techniques below, used fuel content would have to be extracted and converted into a solution for analysis. Though not a technical challenge, fuel dissolution would merely require additional preparatory steps prior to analysis.

Mass Spectrometry

Mass spectrometry identifies elements by converting molecules to ions and then measuring the mass-to-charge ratio of the ions [23] [24] [25] [26] [27]. Traditional mass spectrometry techniques require relatively large sample sizes and can take days or weeks to obtain results, which is less than ideal for facilities with short material balance periods [28]. This includes techniques such as thermal ionization mass spectrometry (TIMS) and inductively coupled plasma mass spectrometry (ICP-MS). However, a technique called laser ablation multi-collector inductively coupled plasma mass spectrometry (LA-MC-ICP-MS) offers the advantage of requiring smaller sample sizes and has been shown to be a rapid mass spectrometry technique that does not require the same chemical preparation as other techniques [29]. In this technique, the laser is used to ablate a small sample that can then be used in the ICP-MS. Mass spectrometry is generally considered to be a mature technique that has high capital and operational costs. It is considered the gold standard for measurement precision, but results take a considerable amount of time to acquire. With the relatively short half-lives of the protactinium isotopes, this technique may not be applicable due to radioactive decay during sample preparation.

Gravimetry

Gravimetry measures the weight of a substance, which in turn can be correlated to mass. There are four main types of gravimetry: precipitation gravimetry, volatilization gravimetry, particulate gravimetry, and electrogravimetry [30]. Precipitation gravimetry relies on the addition of a precipitant to a solution containing the analyte. Once the precipitate and analyte react and precipitation occurs, the precipitate is separated from the solution and analyzed. For large samples, a relative error of 0.1 – 0.2% is generally reached with a precision of several parts per million. This technique is well-known and inexpensive; however, it is time intensive. With newer techniques available, precipitation gravimetry is becoming less commonly used. Volatilization gravimetry involves thermally or chemically decomposing the sample and measuring the change in mass during this process. Volatilization gravimetry has similar accuracy and precision to precipitation gravimetry; however, it is also a time-intensive technique. Particulate gravimetry separates an analyte that is already in a form that is easy to remove from the mixture without the need of a chemical reaction. This separation can be done through filtration or extraction. This technique also generally has the same accuracy and precision as precipitation and volatilization gravimetry. Electrogravimetry uses an electrode and the application of a current or potential [31]. The electrode is weighed before and after the current or potential is applied. The concentration of the analyte can be determined through this change in mass of the electrode. In general, gravimetry techniques are quite mature and precise, but they can be time-intensive and impractical for a large number of samples [32]. With the relatively short half-lives of the protactinium isotopes, gravimetry is not a preferred technique as the ratios of the isotopes may significantly change during the measurement.

Non-Destructive Assay (NDA) Techniques

According to the IAEA Safeguards Glossary, non-destructive assay is "a measurement of the nuclear material content or of the element or isotopic concentration of an item without producing significant physical or chemical changes in the item. It is generally carried out by observing the radiometric emission or response from the item and by comparing that emission or response with a calibration based on essentially similar items whose contents have been determined through destructive analysis [4]." Furthermore, NDA techniques may rely on either passive or induced (i.e., active) measurements for readings and require minimal preliminary sample preparation, unlike the aforementioned DA techniques.

Passive Total Neutron Counting

Passive total neutron counting counts passively emitted neutrons from a sample regardless of their source, time correlation, or initial energy [33]. These neutrons can come from alpha-neutron (α, n) reactions, spontaneous fissions, or self-induced fission, with often small contributions from other background sources. Since ^{233}Pa does not emit neutrons (either via spontaneous fission or alpha-neutron reactions), passive total neutron counting is not a suitable technique for measuring ^{233}Pa.

Passive Neutron Coincidence Counting

Radionuclides that spontaneously fission create neutrons in multiples (doubles and triples) with neutron multiplet signatures that can be isolated from other neutron sources, such as alpha-neutron reactions [28]. This technique works well for radionuclides with a relatively high probability of spontaneous fission, such as some plutonium isotopes, californium, and curium.

However, as previously mentioned, ^{233}Pa does not spontaneously fission nor does any of its decay products. Therefore, this technique will not work for the measurement of ^{233}Pa.

Active Neutron Interrogation

For some materials that do not spontaneously fission nor produce neutrons, it is possible to interrogate the sample with an external neutron source to induce fissions. There are several neutron interrogation techniques. One technique is to use active well coincidence counters (AWCCs) which consist of a sample cavity surrounded by ^{3}He tubes embedded in polyethylene blocks with an (α, n) neutron source located at either end (or both ends) of the cylindrical shaped sample cavity [34]. Another active neutron interrogation technique uses a californium source to induce fission in a sample for a short amount of time. After removing the source, delayed neutrons are counted and correlated to effective fissile mass. All active neutron interrogation techniques are unlikely to provide useful information when measuring ^{233}Pa samples due to the nuclide's relatively small fission cross section (even at neutron energies above 1 MeV). This can be seen in Figure 6, which displays the neutron-induced fission cross section for ^{233}Pa along with that of ^{235}U for comparison.

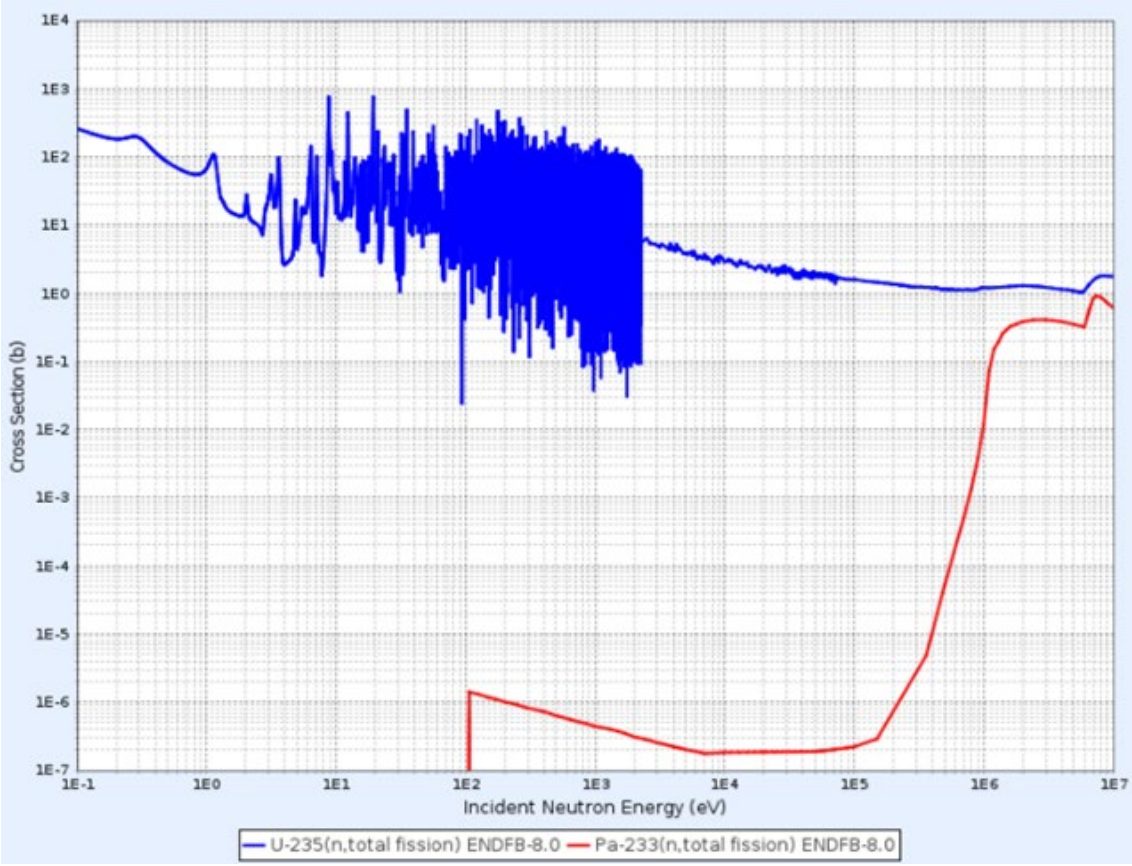

Figure 6: Induced fission cross section for ^{233}Pa (lower red curve) and ^{235}U (upper blue curve) [35].

Hybrid K-Edge Densitometry (HKED)

Hybrid k-edge combines x-ray fluorescence (XRF) and k-edge densitometry (KED). KED works by passing x-rays above and below the k-absorption energies for elements of interest in the measurement sample [28] [36]. The size of the discontinuity at the k-absorption edge can be correlated to the concentration of the element. XRF can be used to measure the intensity of induced x-rays in the measurement sample, thus quantifying the total mass of the element of interest in the sample. The combination of these two techniques lowers the measurement uncertainty and allows for the absolute concentration of each element to be determined. This technique is promising since it can be used onsite and could allow for close to real-time measurements. Precision of ~0.5% can be achieved with measurement durations of 5-20 minutes [37]. HKED is a mature technology with

commercial systems available; however, the costs of these systems are moderate to high and require a moderate amount of floor space. This technique measures elemental masses and not isotopic masses, which may be required based on the material accountancy requirements.

Laser-Induced Breakdown Spectroscopy (LIBS)

Laser-induced breakdown spectroscopy works by hitting a small portion of the sample material with a laser producing a high-energy plasma [38]. As the plasma cools, atoms relax from excited states back to ground states and emit light. LIBS spectral analysis can determine the elements emitting each spectral peak. Advantages to this technique include minimal preparation time of samples and the ability to obtain near real time results. Using this method directly on liquid molten salt may present challenges due to splash back on the optical equipment as the laser hits the surface of the liquid [39]. A newer LIBS technique forms a molten salt aerosol to then hit with the laser to reduce the splash back effects. This technique is not mature yet and needs more research and development before it can be conclusively determined as a possible technique for ^{233}Pa assay. It also can be noted that LIBS is not entirely an NDA technique since a small portion of the material is destroyed during the measurement process.

Calorimetry

Calorimetry is a technique of measuring heat produced by different materials during chemical processes to determine the mass [40] [41] [42]. This technique has been used for around 45 years and has become a primary technique in the United States for the assay of plutonium and tritium for nuclear material accountability [43]. While this technique is commonly used and quite accurate, it takes a relatively long time to acquire results compared to other NDA techniques. As previously mentioned, ^{233}Pa has a half-life of 27 days, and the other protactinium isotopes have

even shorter half-lives. With the time delay of results, the relative concentrations of the protactinium isotopes can change by a significant amount. Although calorimetry is a mature technique, a quicker technique is required, thus making calorimetry impractical for the purpose of measuring protactinium.

Passive Gamma Spectroscopy

Gamma spectroscopy measures the gamma-ray emissions and their energy distribution from radionuclides when they undergo radioactive decay [44] [45]. Each radionuclide has its own unique gamma spectrum that can aid in the identification of the nuclide. Some radionuclides have a clear gamma spectrum with high yield gamma lines that are well separated in energy, while others can have complicated gamma spectra that are difficult to use for identification due to only a few gamma lines with low yields that are closely spaced in energy with each other or gammas from other radionuclides. Radionuclides that have a clear gamma spectrum with distinct high yield gamma energies are easy to use for identification. Radionuclides that have more complicated gamma spectra are difficult to use for identification due to having only a few low yield gamma energies that may be closely spaced with each other or gammas from other radionuclides. Gamma spectroscopy is a mature technique, can be fairly cheap when compared to other NDA measures (especially when using a NaI detector), and produces results relatively quickly (within minutes). The precision of gamma spectroscopy ranges with the detector material used and the nuclear material being measured. Sodium iodide (NaI) detectors have low energy resolution but are inexpensive and can operate at room temperature. High-purity germanium (HPGe) detectors have higher energy resolution but require very low operating temperatures (about 77 K) and exhibit sensitivity to neutron damage. In-field usage of HPGe detectors can create additional engineering challenges depending on the facility layout and operational plan. In addition to HPGe detectors

being noticeably more expensive in comparison, NaI detectors are generally easier to model despite requiring often recalibration due to the tendency of energy calibration drift with changing environmental conditions. Often gamma spectroscopy is used to acquire isotopic ratios, which when combined with other NDA techniques such as neutron multiplicity counting, can provide isotopic masses in a sample. In particular, ^{233}Pa exhibits several characteristic high intensity gamma peaks, of which five can be used for signifying presence (due to probabilities of emission with over 1% yield): 300 keV, 312 keV, 340 keV, 398 keV, and 416 keV. With these five peaks, the gamma spectrum of extracted ^{233}Pa could be easily identified, assuming minimal background radiation. The need for longer measurement times due to low count rates is not expected since ^{233}Pa has a specific photon emission rate (gamma rays created per second per gram) of 1.0×10^{15}. This is almost eight orders of magnitude larger than that of ^{233}U at 2.5×10^{7}. For these reasons, the gamma spectroscopy technique was the primary focus in this research for measuring ^{233}Pa in the separated protactinium mixture from thorium-based fuels.

1.4. Codes Used

Various codes were used throughout this research. Monte Carlo N-Particle (MCNP) code version 6.2 was used along with RadSrc to simulate the initial gamma spectra of the protactinium isotopes and the daughter products all separately [46] [47]. MCNP is a Monte Carlo radiation transport code developed by Los Alamos National Laboratory. RadSrc is a library developed by Lawrence Livermore National Laboratory used to calculate radioactive decay product concentrations given an initial isotope mixture and age.

To create a mixed gamma spectrum of the protactinium isotopes and their decay products as would be seen from used nuclear fuel, Oak Ridge Isotope GENeration 2 (ORIGEN2) was used in conjunction with the MCNP simulations [48]. ORIGEN2 is a well-established reactor burnup code that is relatively easy

to use and provides computations on the order of seconds. It is also advantageous because it captures the full core, rather than just an individual fuel pin or assembly. The primary disadvantage of ORIGEN2 is that it has not been updated since June of 2002 and is only validated for certain fuel compositions [49]. Fuel compositions outside of its validation range could create a neutron energy spectrum different from the model, thus leading to inaccurate used fuel compositions.

After using ORIGEN2 for burnup calculations, MCNP was used for burnup calculations as a comparison to verify the accuracy of the ORIGEN2 results. In contrast to ORIGEN2's zero-dimensional point models, MCNP allows for three dimensional geometries. MCNP also does not make any assumptions about the neutron energy spectrum, but instead recalculates the spectrum for each time step based on the current fuel composition. This allows for any fuel composition to be simulated and for the simulations to be valid for a wider range of burnups. MCNP is continually being updated, with the newest 6.2 version being released in 2018 [46]. The primary disadvantage of MCNP is that the input to the simulation can take more time to create and the execution of the code takes longer, especially for burnup simulations. To decrease the length of these simulations and the complexity of the input, often only a single pin or a fuel assembly is modeled. Reflective boundary conditions can be included to create an infinite array of fuel pins, which is valid for pins in the center of the reactor but will produce incorrect results for pins on the outer edge of a reactor. Because of these reasons, both ORIGEN2 and MCNP 6.2 burnup simulations were performed.

MSRs using liquid fuel require more complex modeling and simulation than PWRs and CANDU reactors due to the fact that the fuel is continuously flowing though the core region. This dynamic nature cannot be properly modeled yet by established, widely-used fuel burnup codes. Because of this, the Transport Rigor Implemented with Time-dependent Operation for Neutronic depletion (TRITON) sequence of the in-development beta version 16 of the Standardized

Computer Analyses for Licensing Evaluation (SCALE) 6.3 was used to allow for continuous flow of the fuel in the MSR [49]. SCALE was developed by Oak Ridge National Laboratory as a modeling and simulation suite for nuclear safety analysis and design [50]. TRITON is a SCALE module designed for 2-D and 3-D depletion calculations utilizing cross-section processing codes, a neutron transport solver, and ORIGEN [51].

1.5. Layout of Thesis

This thesis is comprised of four major sections. The first section covered motivations and objectives, as well as necessary background information required for this research. The second section describes the methodology carried out for this work. The methodology explains the different simulations ran to generate gamma spectra for protactinium separated from used fuel. The third section discusses and evaluates the results obtained in the second section. The fourth section concludes the thesis and identifies possible future work for this research.

2. METHODOLOGY

2.1. MCNP Gamma Spectra Generation

To understand protactinium gamma spectra, radiation transport detector measurements were simulated using MCNP. Specifically, ^{232}Pa, ^{233}Pa, and ^{234}Pa, along with their decay products (^{208}Tl, ^{212}Bi, ^{212}Pb, ^{216}Po, ^{220}Rn, ^{224}Ra, ^{225}Ra, ^{226}Ra, ^{228}Ra, ^{228}Th, ^{229}Th, ^{230}Th, ^{232}Th, ^{232}U, ^{233}U, ^{234}U) were simulated separately. The software RadSrc was used to generate the discrete gamma line energies needed for the source definition in the MCNP simulations. The configuration of each simulation consisted of a point source of the radionuclide and a detector with its front face located 10 cm away. Two different types of detectors were simulated: a 2”x2” NaI crystal-based detector and a 2”x2” HPGe coaxial detector.

Simulating each radionuclide separately allowed the unique gamma spectrum to be clearly shown for each individual radionuclide. These spectra can then be compared to a more realistic mixed source to identify the radionuclides that are present in the source. Referring to the ^{233}Pa spectrum in Figure 7, certain gamma energies have high intensities and aid in the identification of this radionuclide. The gamma spectra for ^{232}Pa and ^{234}Pa are included in Appendix A.

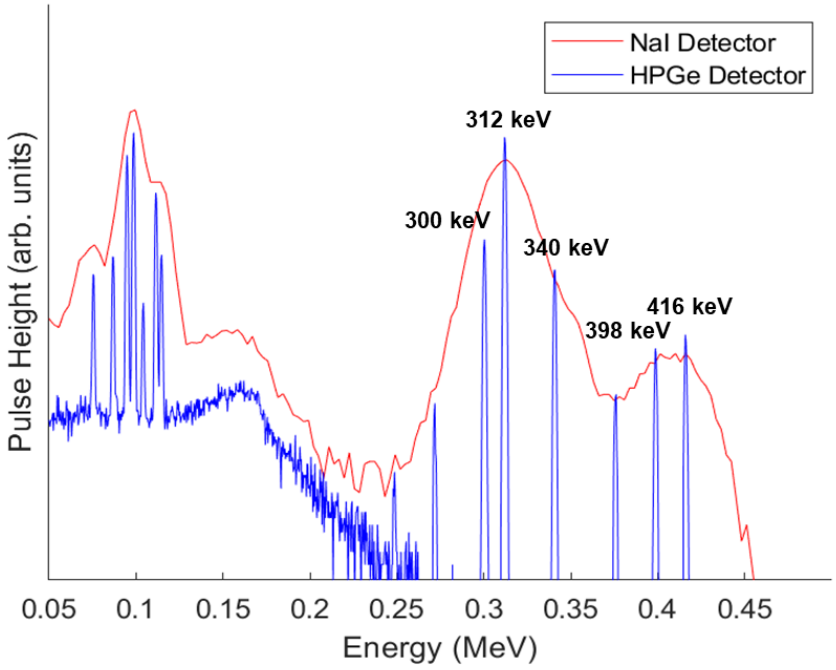

Figure 7: Gamma spectrum for ^{233}Pa showing high intensity energies most notably at 300 keV, 312 keV, 340 keV, 398 keV, and 416 keV. This gamma spectrum was produced using both a NaI detector (red) and a HPGe detector (blue) in MCNP.

2.2. ORIGEN2 Burnup

To create a mixed source with the correct isotopic distribution of protactinium isotopes, nuclear reactor simulations were created using MCNP and ORIGEN2. Four different reactor types were modeled in ORIGEN2 [48] to simulate burnup. The first reactor modeled was a mixed thorium/uranium oxide-fueled PWR (called PWRUS in ORIGEN2) with an actinide mixture of

80% Th and 20% U with an enrichment of 19.9% ^{235}U and a burnup of 47 GWd/MTHM [52]. The second reactor was also a PWR (called PWRD5D35 in ORIGEN2) with the same inputs but a slightly different neutron energy flux profile. This fuel composition was chosen because it has approximately the same initial fissile atom density (^{235}U) as fuel with a 100% uranium actinide content but an enrichment of only 4% ^{235}U. In theory, higher uranium enrichments could be used to further reduce the mass of uranium while still maintaining the initial fissile atom density, but enrichments at or above 20% are considered highly enriched uranium (HEU) and create additional proliferation concerns. For the third reactor, a CANDU (called CANDUNAU in ORIGEN2) reactor was used with 19% Th and 81% U with an enrichment of 0.71% ^{235}U. This reactor had a burnup of 19 GWd/MTHM. This fuel composition represents the limits of how much thorium can be added to natural uranium while still maintaining criticality in a CANDU style reactor. Lastly, another CANDU (called CANDUSEU in ORIGEN2) reactor was modeled with 91% Th and 9% U with an enrichment of 20% ^{235}U and a burnup of 14 GWd/MTHM [53]. Each of the reactor simulations were set to return fuel composition values for continuous durations of 0, 0.1, 1, 3, 10, 30, 100, and 300 days after reactor shut down. For each of these time steps, a different protactinium composition was observed. This represents what the protactinium composition would look like if reprocessing took place at different decay times. While it is unrealistic to think that PWR or CANDU fuel can be reprocessed immediately after discharge, a simulation of this type does provide data points allowing for interpretation and extrapolation for extreme situations. These extracted protactinium quantities were all plotted for each reactor type over time from immediate discharge to 300 days. The graphed ORIGEN2 output for the PWRUS is shown in Figure 8. The output for the other reactors can be seen in Appendix B.

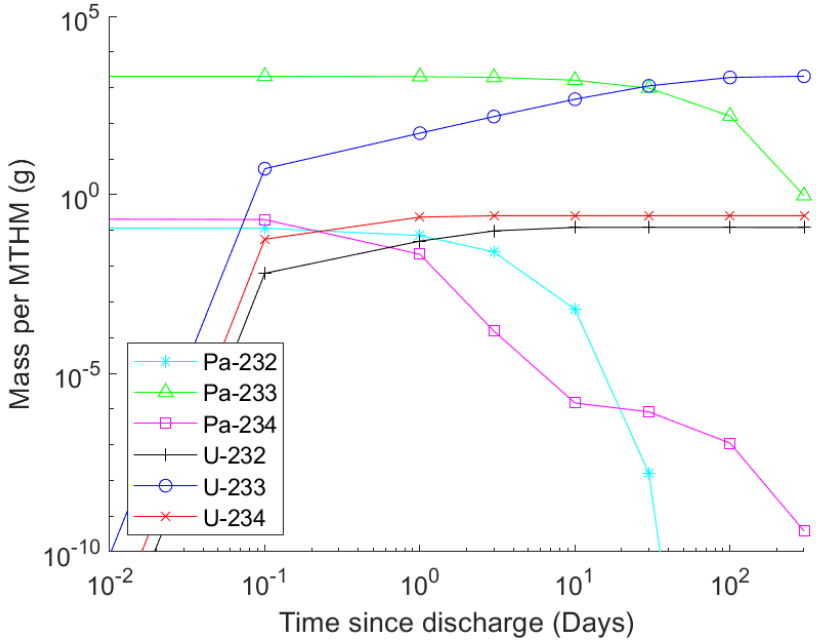

Figure 8: Relative abundance of the separated protactinium isotopes and the uranium produced from decay present in the separated fuel from soon after discharge to 300 days post-discharge for the PWRUS.

The MCNP radiation detector simulation spectra and the ORIGEN2 simulation of protactinium mass quantities in the used fuel were then combined to create the mixed gamma spectrum of only ^{232}Pa, ^{233}Pa, and ^{234}Pa and their decay products, representing what a gamma spectrum of extracted protactinium from the used fuel would look like. Gamma spectra were produced for the isolated protactinium mixture at each of the time steps generated using the ORIGEN2 simulations. An example of this can be seen in Figure 9 for the PWRUS at all of the simulateed time steps. Only protactinium isotopes were present at 0 days due to the lack of decay products. Progressing through the time steps shows the protactinium decaying and the daughter products building up.

a)

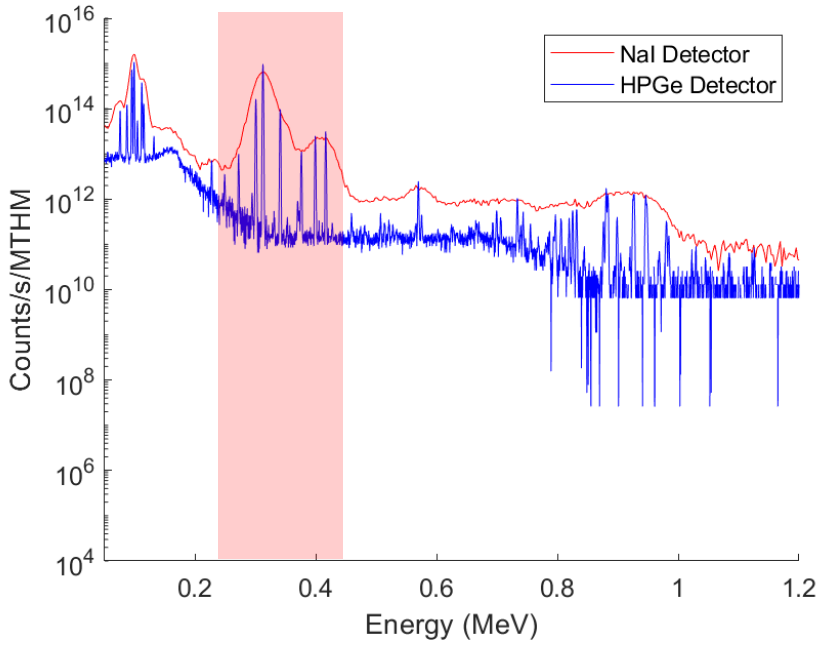
NaI Detector
HPGe Detector
Counts/s/MTHM
Energy (MeV)
10^{16}
10^{14}
10^{12}
10^{10}
10^{8}
10^{6}
10^{4}
0.2
0.4
0.6
0.8
1
1.2

b)

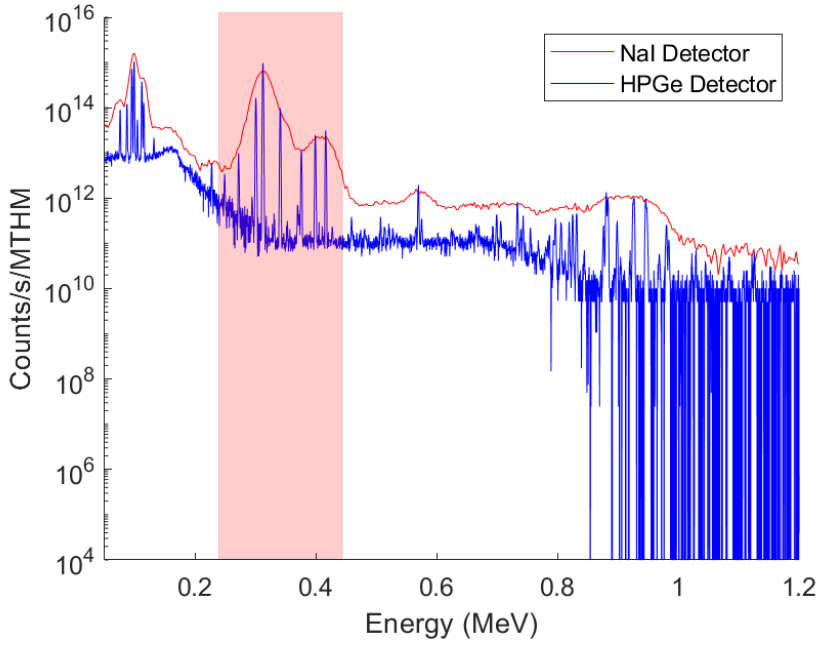
NaI Detector
HPGe Detector
Counts/s/MTHM
Energy (MeV)
10^{16}
10^{14}
10^{12}
10^{10}
10^{8}
10^{6}
10^{4}
0.2
0.4
0.6
0.8
1
1.2

c)

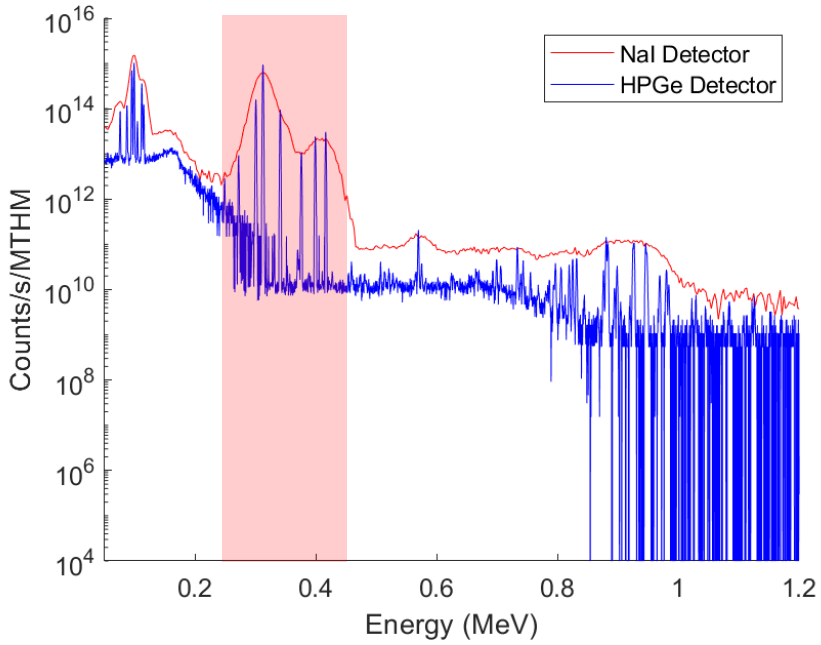
NaI Detector
HPGe Detector
Counts/s/MTHM
Energy (MeV)

d)

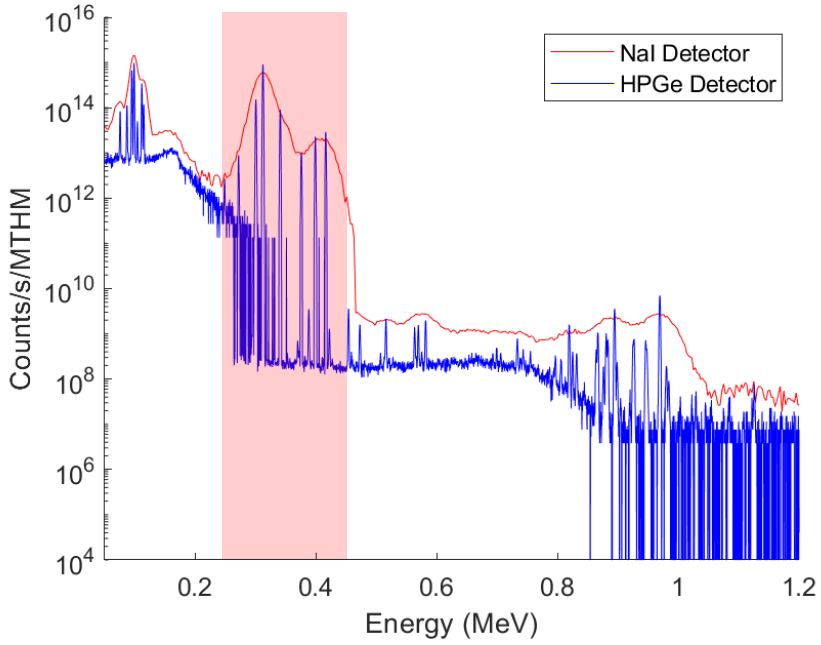
NaI Detector
HPGe Detector
Counts/s/MTHM
Energy (MeV)

e)

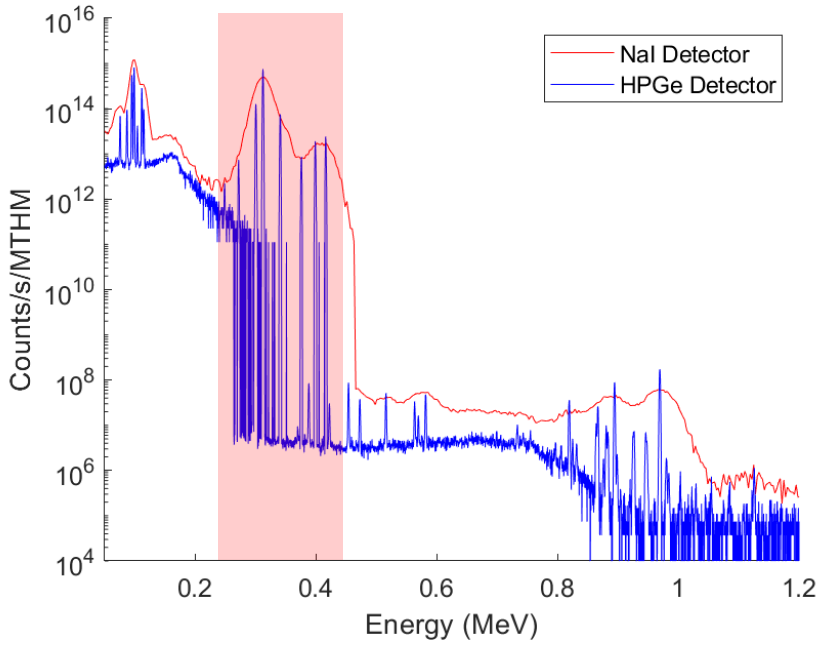
NaI Detector
HPGe Detector
Counts/s/MTHM
Energy (MeV)

f)

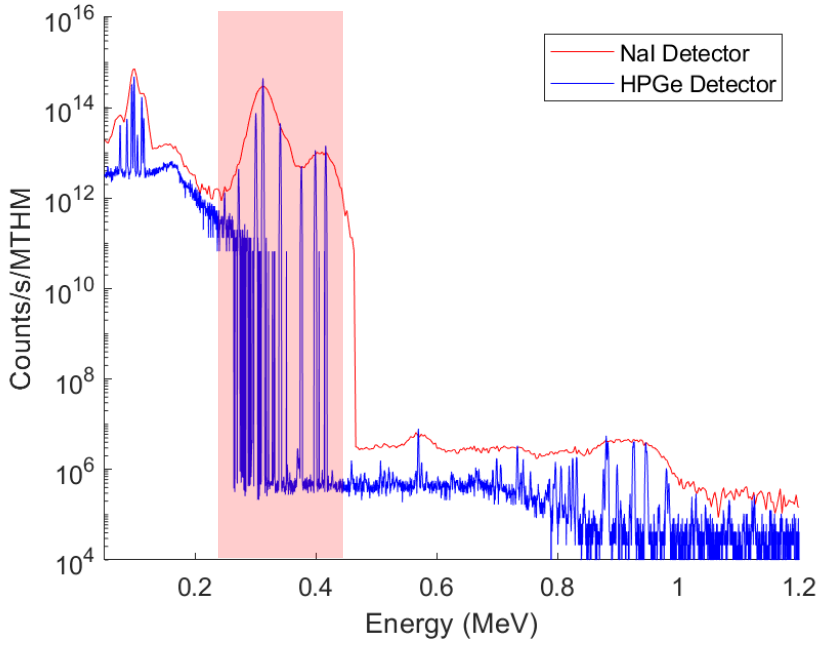
NaI Detector
HPGe Detector
Counts/s/MTHM
Energy (MeV)

g)

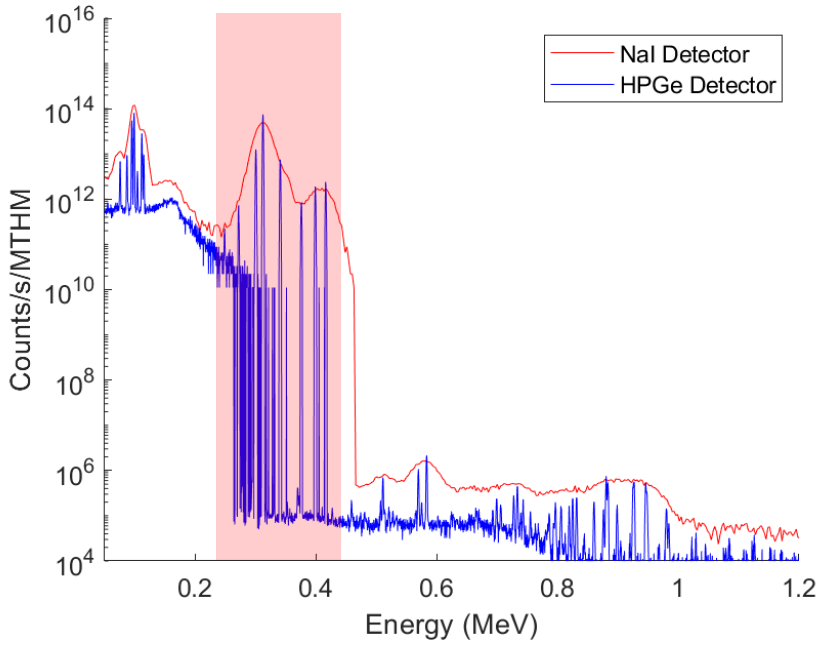

h)

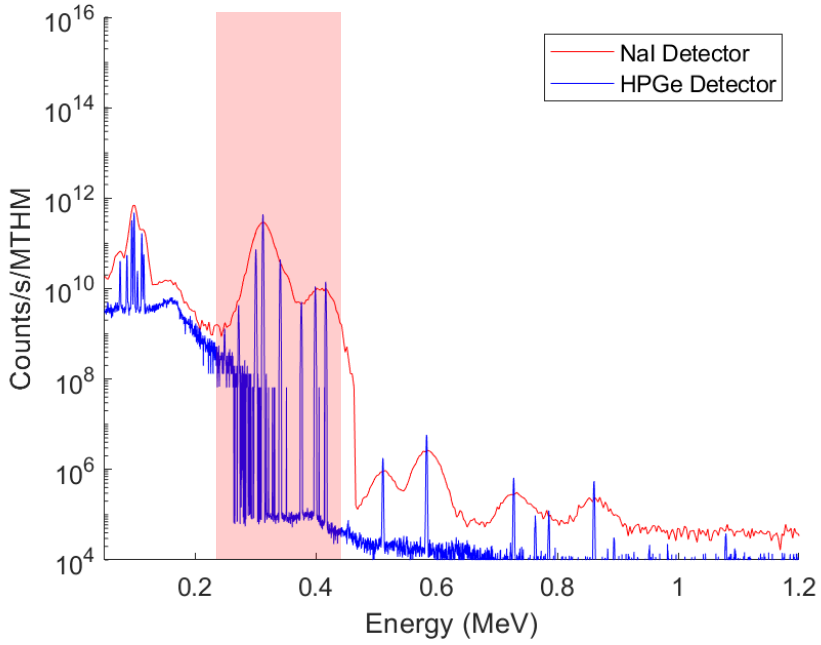

Figure 9: Gamma spectrum of the isotopes for the PWRUS reactor in the MCNP/ORIGEN2 simulations at (a) time of discharge, (b) 0.1 days, (c) 1 day, (d) 3 days, (e) 10 days, (f) 30 days, (g) 100 days, and (h) 300 days. This gamma spectrum was produced using both a NaI detector (red) and a HPGe detector (blue) in MCNP. Relevant ^{233}Pa peaks are highlighted within the red boxes.

2.3. MCNP Burnup

The next step in the research was to simulate the burnup of a PWR and two CANDU reactors using MCNP. The PWR was modeled as a single fuel rod, shown in Figure 10, with mirrored boundaries to create an infinite array of fuel rods. The modeled dioxide fuel had an actinide content of 80% Th and 20% U, with the uranium being 19.7% enriched. The fuel was burned for 1150 full power days with the following time intervals in days: 0.1, 0.2, 0.4, 0.5, 0.8, 1, 2, 4, 8, 16, 25, 50, 75, 100, 100, 100, 100, 100, 100, 100, 100, 167. The fuel and gap temperatures were modeled at 900 K with that of the cladding and water at 600 K. The neutron light water moderation treatment was used for the water and its density adjusted to 0.717 g/cm^3 to account for the elevated temperature and pressure of PWR primary coolant. K-code simulations were performed with 1000 particles per cycle, 2000 cycles, and excluding results from the first 50 cycles due to potential biasing in neutron starting locations.

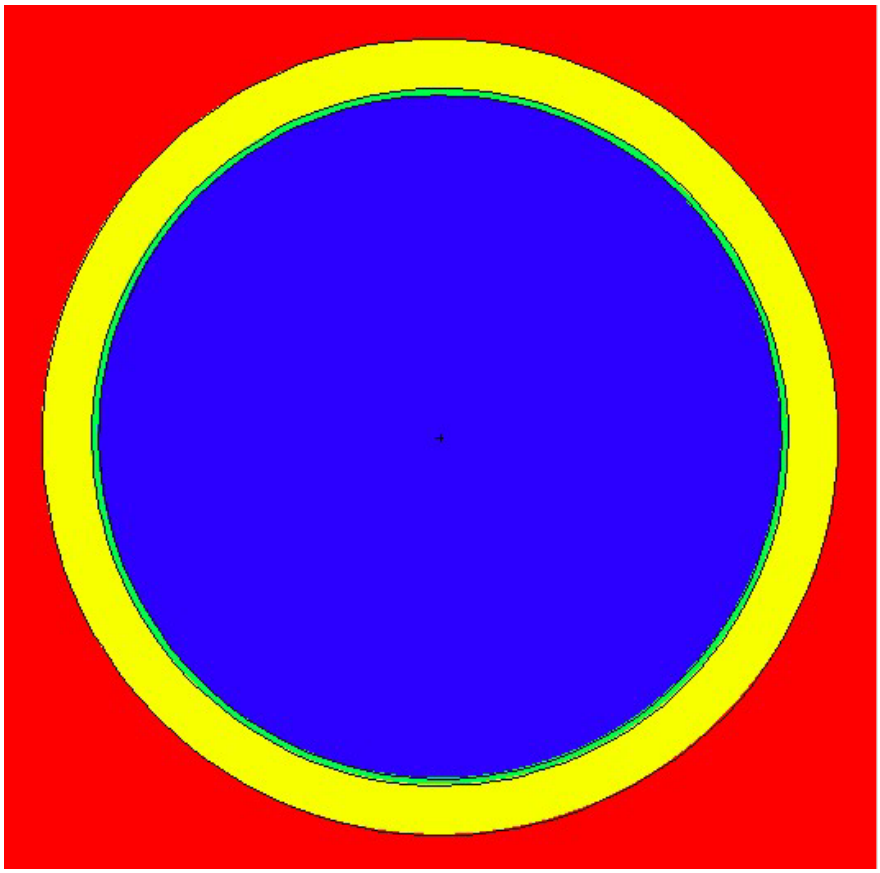

Figure 10: Axial view of the modeled PWR fuel rod. The fuel region is shown in blue, surrounded by a thin helium gap (green) followed by the zircaloy-4 cladding (yellow), which is surrounded by light water (red).

Both CANDU reactors were modeled as single fuel assemblies with mirrored boundaries, as shown in Figure 11. The first CANDU used U-Th-O_2 fuel with natural uranium and 19% of the fuel's actinide content being thorium. The second CANDU model used U-Th-O_2 fuel with 19.7% enriched uranium and 91% of the fuel's actinide content being thorium. The fuel was burned for 365 full power days with the following time intervals in days: 0.1, 0.2, 0.4, 0.5, 0.8, 1, 2, 4, 8, 16, 25, 50, 75, 91, 91. The temperatures were the same as the PWR model and the neutron heavy water moderation treatment was used for the water. The heavy water had a density of 0.836 g/cm^3 to account for the elevated temperature and pressure of CANDU reactors. K-code simulation parameters were the same as those for the PWR simulations.

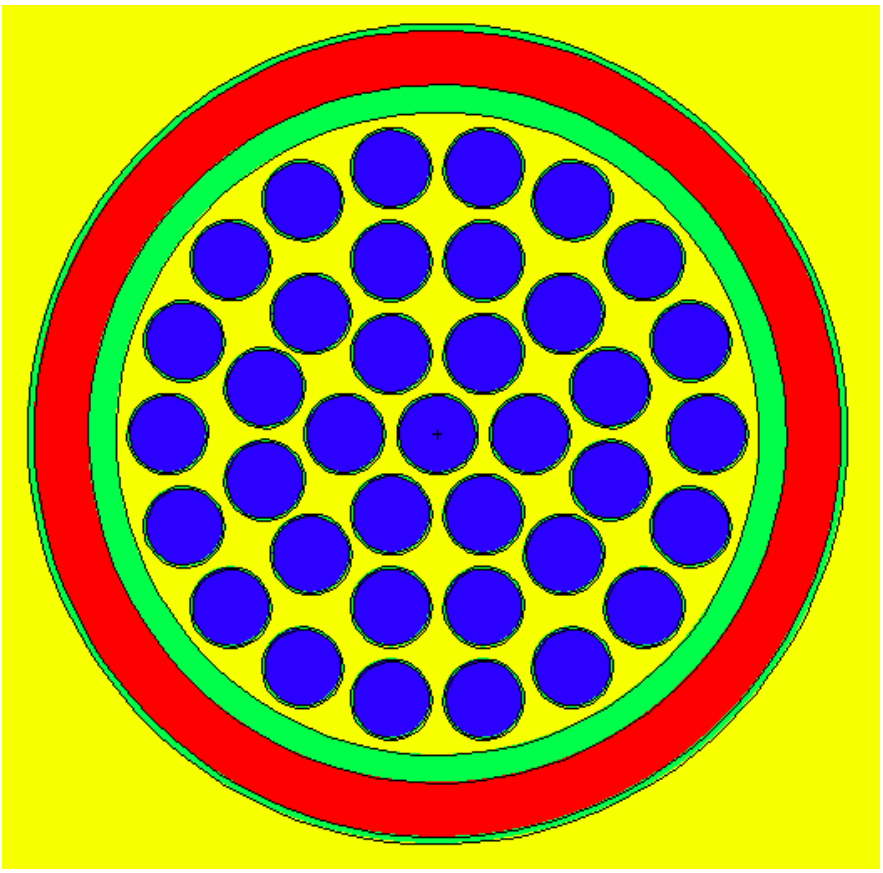

Figure 11: Axial view of the modeled CANDU fuel assembly. The fuel region is shown in blue, surrounded by the Zircaloy-4 cladding (black), which is surrounded by heavy water (yellow). These fuel rods and coolant are encased in a cylindrical pressure tube of Zircaloy-4 (green), followed by a think helium gap (not shown), then a cylindrical calandria tube of Zircaloy-4 (red), all surrounded by heavy water (yellow).

The gamma spectra for the generated protactinium isotopes and their decay products for each reactor were then produced for the same decay time steps as the previous simulations (0, 0.1, 1, 3, 10, 30, 100, and 300 days). Figure 12 shows the gamma spectrum for the extracted, elemental protactinium from the PWR at 0 days and 300 days. The gamma spectra for the other time steps and other reactor models for the MCNP simulations can be found in Appendix D.

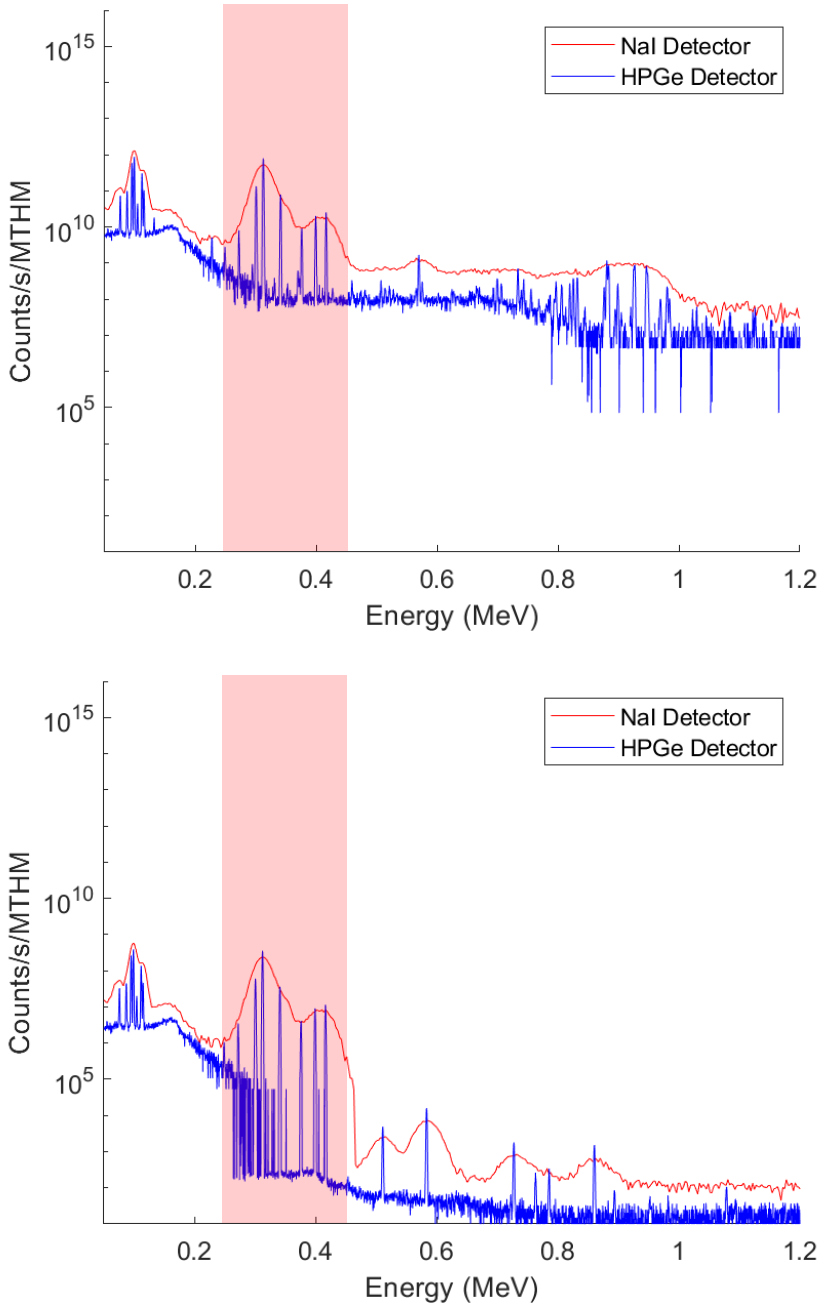

Figure 12: Gamma spectrum of the isotopes for the PWR using the MCNP stand-alone simulation at time of discharge (top) and after 300 days (bottom). This gamma spectrum was produced using both a NaI detector (red) and a HPGe detector (blue) in MCNP. Relevant ^{233}Pa peaks are highlighted within the red boxes.

2.4. SCALE Triton

Due to the availability of design specifications, the single-fluid double-zone thorium-based molten salt reactor (SD-TMSR) design was chosen as the representative MSR core [54] with simulated continuous online reprocessing and refueling. The active core of this reactor has two main radial regions, the inner zone and the outer zone, in a hexagonal graphite matrix, as shown in Figure 13. The inner zone is composed of 486 relatively small fuel channels (3.5 cm radius) and the outer zone is composed of 522 larger fuel channels (5 cm radius). The two regions have the same channel pitch which results in different fuel to moderator ratios in the two regions and allows for control over the breeding performance of the design. The core is designed to have a radial graphite reflector and surrounding cylindrical B_4C shielding and Hastelloy containment, however these regions were modeled as a single hexagonal graphite region extending 48.65 cm beyond the active region. The fuel salt is modeled as a lithium-beryllium fluoride salt carrying ^{232}Th and ^{233}U and with 100% ^{7}Li purity. The initial fuel salt composition of LiF-BeF_2-Th F_4-$^{233}UF_4$ was modeled as 11.66-10.67-60.41-17.26 wt% (about 44% ^{232}Th and 0.78% ^{233}U). The first 1500 days of operation of the reactor were modeled, during which it was to maintain a specific power of 52.711 MW/MTHM. During the simulation, the active region had material flows designed to model the removal of material through reprocessing and the reintroduction of new fuel material. The flows were constructed to remove fission products and non-dissolved metals at a rate of 3.333×10^{-2} s^{-1} and actinides at a rate of 1.092×10^{-6} s^{-1}. Protactinium was also removed to a separate tank at a rate of 1.092×10^{-6} s^{-1}. ^{232}Th and ^{233}U were added back into the system at net rates normalized to the initial core inventory in kg-HM. During the first 90 days of operation the normalized net rates of ^{232}Th and ^{233}U were 2.021×10^{-6} g/s and 1.421×10^{-6} g/s, respectively. For the remaining simulation time, these rates were adjusted to 1.550×10^{-6} g/s and 2.938×10^{-6} g/s.

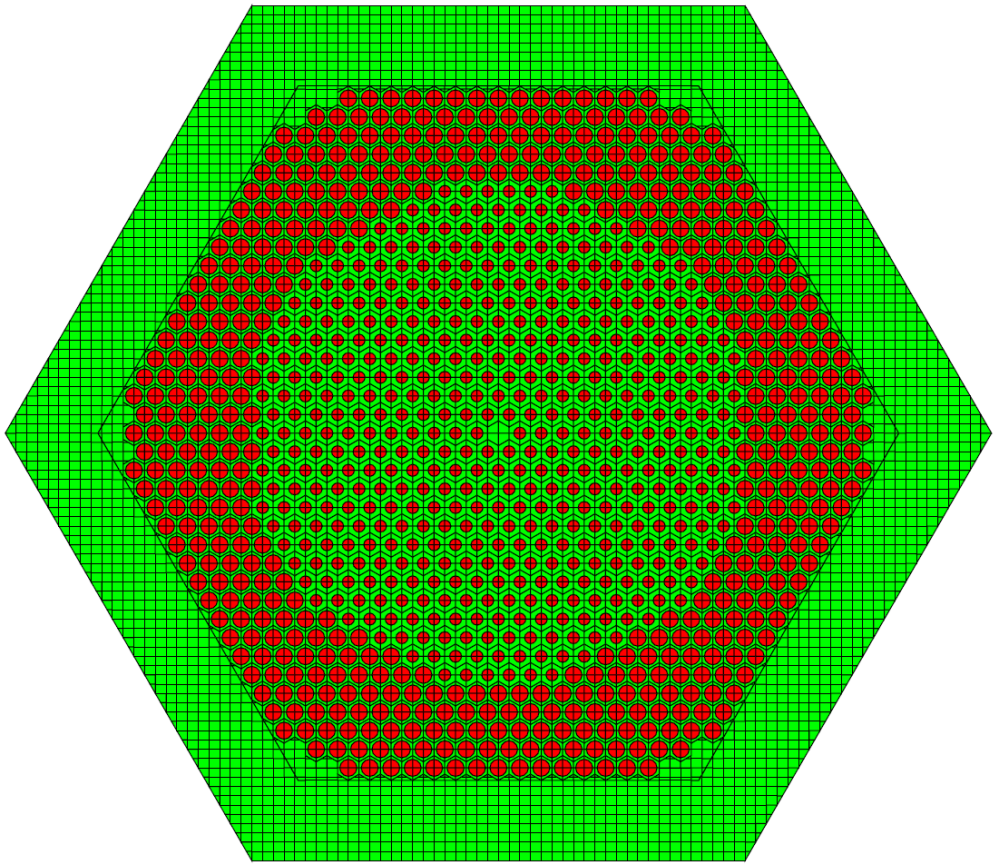

Figure 13: Modeled MSR reactor showing the red fuel region and green graphite moderator.

In order to get a more detailed composition for the protactinium in the decay tank, further modeling was done using standalone ORIGEN-S with the depletion library created in the neutronics simulation. This required a two-step modeling process. In the first step, the reactor fuel composition was calculated using the same initial composition, material removal rates, and new fuel feed rates but with much shorter time steps. From this, the protactinium isotope concentrations in the core were found and thus, with the removal rates of protactinium modeled, the rate that each of the isotopes would be expected to enter the decay tank at each time. In the second step, the protactinium isotopes are modeled to flow into an initially empty tank with stepwise constant flow rates equal to the average flow rate for that time step. In the tank, the protactinium is allowed to decay over the 1500 days modeled with zero incident flux and all non-protactinium nuclides

assumed to be removed. The mass concentration for ^{232}Pa, ^{233}Pa, and ^{234}Pa in the tank can be seen in Figure 14. Figure 15 shows the mass concentration for ^{232}Pa, ^{233}Pa, and ^{234}Pa in the tank during only the first 100 days to better show the initial increase of the isotopes to the eventual equilibrium in the tank.

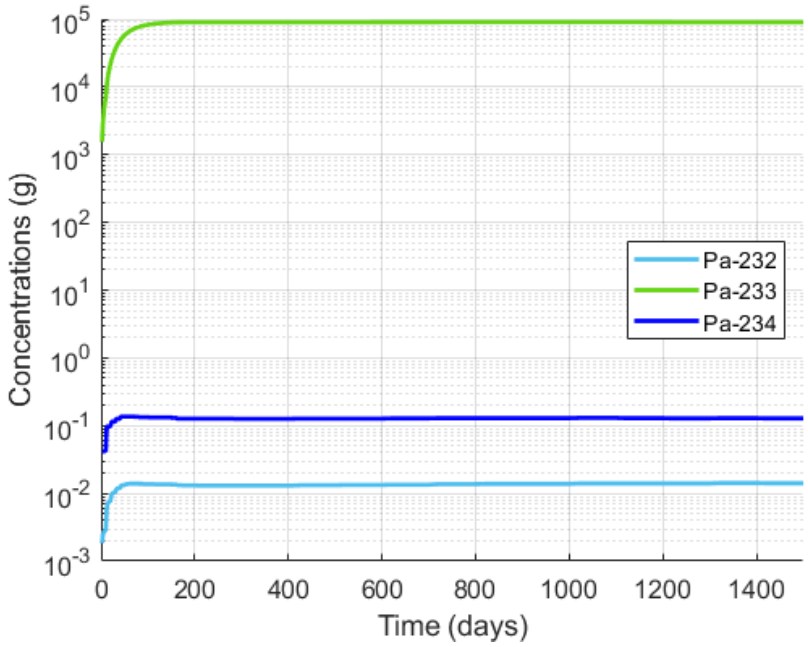

Figure 14: Mass concentration for ^{232}Pa, ^{233}Pa, and ^{234}Pa in the tank over time.

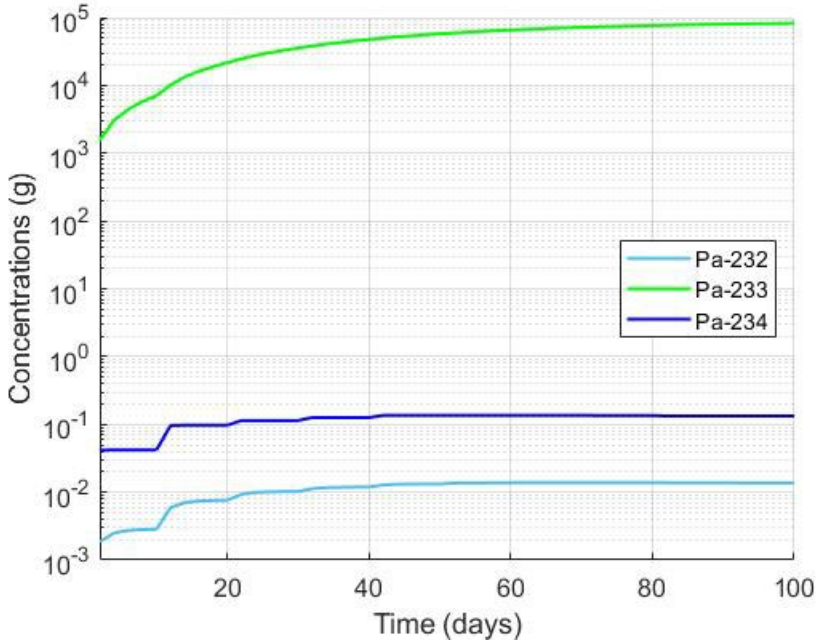

Figure 15: Mass concentration for ^{232}Pa, ^{233}Pa, and ^{234}Pa in the tank over the first 100 days.

The gamma spectra from the separated elemental protactinium in the tank were produced for the MSR at 2, 10, 30, 100, and 300 days. The gamma spectra for all of the simulated time steps are shown below in Figure 16. Unlike the other simulated reactors, the protactinium isotopes are shown to increase on the gamma spectra rather than decrease. This is due to the protactinium being continuously added to the same tank when removed from the liquid fuel.

a)

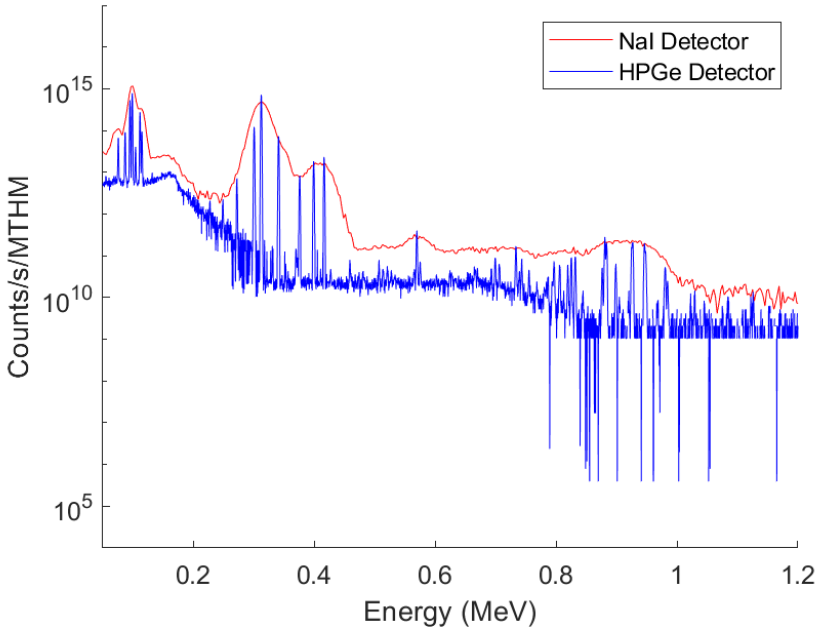
NaI Detector
HPGe Detector
Counts/s/MTHM
10^{15}
10^{10}
10^{5}
0.2
0.4
0.6
0.8
1
1.2
Energy (MeV)

b)

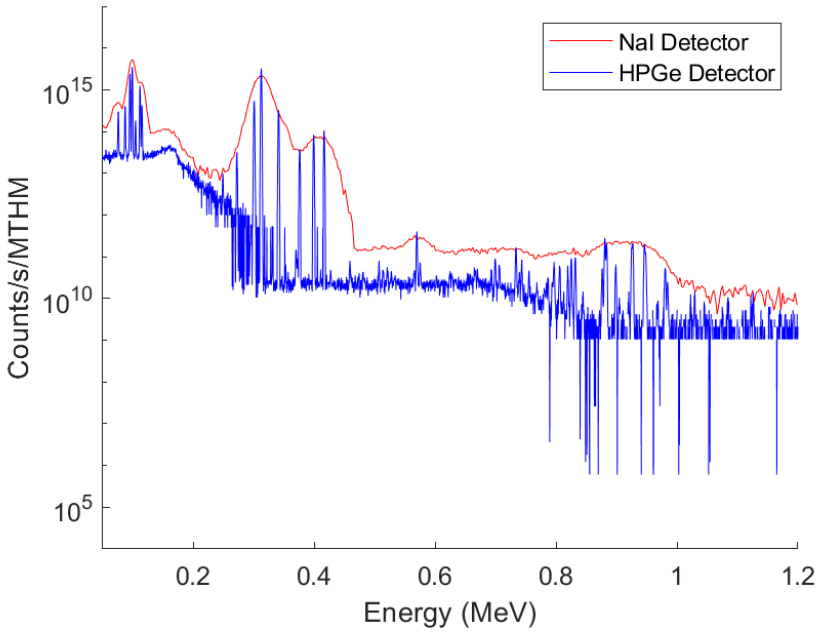
NaI Detector
HPGe Detector
Counts/s/MTHM
10^{15}
10^{10}
10^{5}
0.2
0.4
0.6
0.8
1
1.2
Energy (MeV)

c)

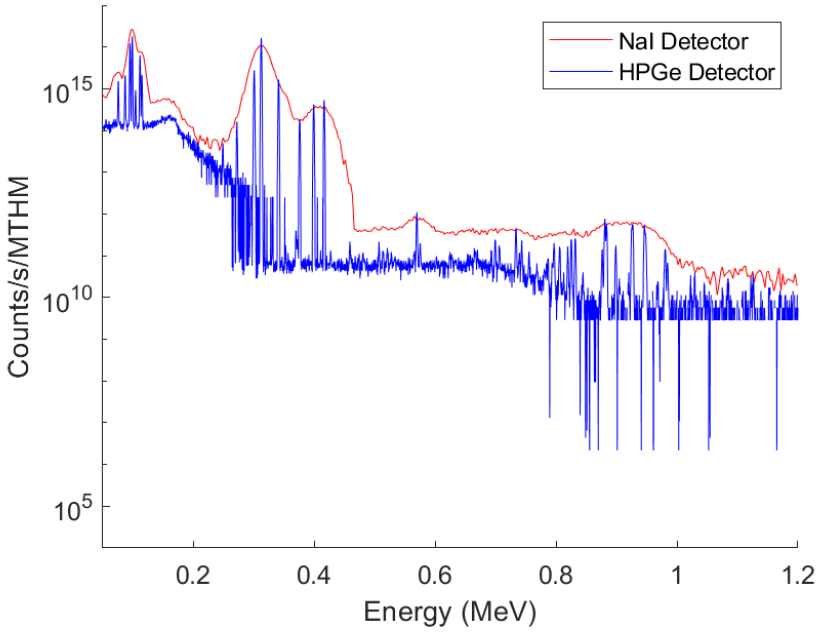
NaI Detector
HPGe Detector
Counts/s/MTHM
10^{15}
10^{10}
10^{5}
0.2
0.4
0.6
0.8
1
1.2
Energy (MeV)

d)

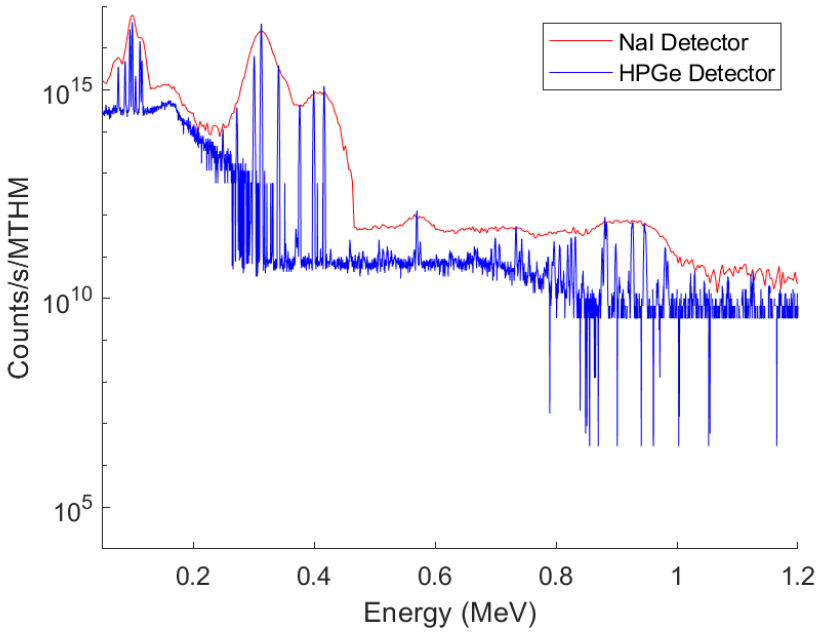
NaI Detector
HPGe Detector
Counts/s/MTHM
10^{15}
10^{10}
10^{5}
0.2
0.4
0.6
0.8
1
1.2
Energy (MeV)

e)

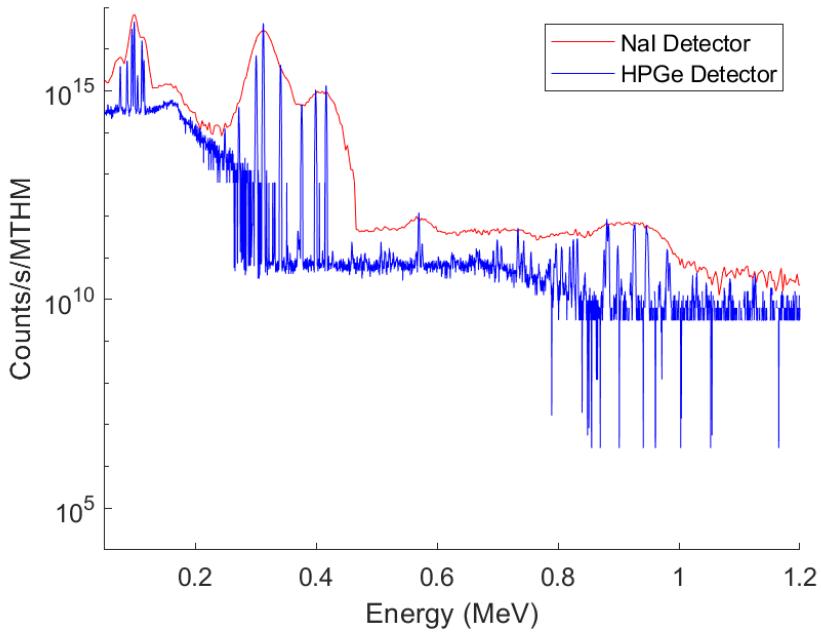

Figure 16: Gamma spectrum of the protactinium in the tank for the MSR using the SCALE Triton simulation after (a) 2 days, (b) 10 days, (c) 30 days, (d) 100 days, and (e) 300 days. This gamma spectrum was produced using both a NaI detector (red) and a HPGe detector (blue) in MCNP. Relevant ^{233}Pa peaks are highlighted within the red boxes.

3. RESULTS AND DISCUSSION

Multiple DA and NDA techniques were reviewed and considered for their applicability to measure ^{233}Pa in an extracted stream of elemental protactinium. This review identified that both HKED and passive gamma spectroscopy are potentially viable techniques that produce timely measurements. Due to the limited scope of this work, however, only passive gamma spectroscopy was evaluated. The spectra shown in Appendix A indicate that both NaI and HPGe detectors can easily identify ^{232}Pa and ^{233}Pa in isotopically pure samples under ideal conditions. The identification of ^{234}Pa may be more challenging due to fewer prominent gamma rays as shown in Figure 17 below.

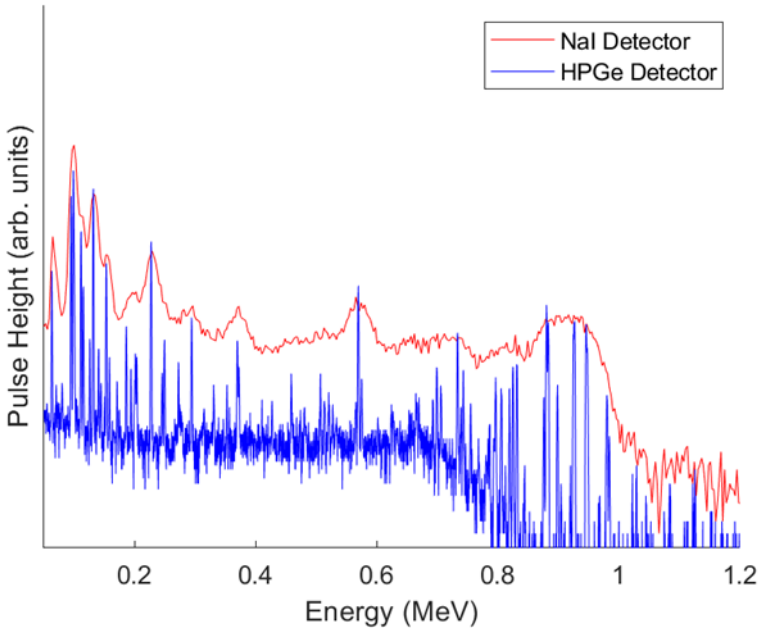

Figure 14: Gamma spectrum for ^{234}Pa.

Because separating isotopically pure samples of protactinium from used fuel is unrealistic, several different reactor types were modeled to generate realistic compositions of the protactinium isotopes. This data, shown in Appendix B, indicates that the protactinium concentrations and compositions at the end of the fuel life for the PWR models are largely independent of slight differences in the neutron flux energy. For the CANDU models, the protactinium mass values show more variation than the PWR data but are still mostly similar with each other. This indicates that the initial fraction of the fuel that is thorium and the initial enrichment of uranium has minimal impact on the protactinium mass values at the end of fuel life. This is likely due to the fact that all isotopes of protactinium have relatively short half-lives and thus do not continuously build up in the used fuel. When comparing the PWRUS and CANDUSEU (both of which use ~20% enriched uranium with most of their initial actinide mass being thorium), there is a noticeable difference in the protactinium masses. The CANDU reactor produces about 10% less ^{232}Pa than the PWR. This

is not surprising since it is known that the concentration of ^{232}U in thorium fuel cycles has a slight dependence on the neutron energy spectrum of the reactor [55].

Gamma spectra were produced from the PWR and CANDU protactinium mass data described above. These gamma spectra can be found in Appendix C for the ORIGEN2 burnup simulations and Appendix D for the MCNP burnup simulations. With respect to decay time, this data shows how the cluster of ^{233}Pa gamma peaks in the 300-400 keV region remain visible for both NaI and HPGe detectors for all simulated decay times. The intensities of these peaks do decrease with decay time due to the relatively short half-life of ^{233}Pa. At zero days (extracting the protactinium from the used fuel immediately after it is discharged from the reactor), the counts from these peaks are approximately 10^{15} counts/s/MTHM/channel for the simulated measurement geometry. This value decreases to approximately 10^{12} counts/s/MTHM/channel after 300 days of decay. There is a lower intensity cluster of peaks in the 800-1,000 keV region that is visible at zero days. These peaks are due to other protactinium isotopes and rapidly drop in intensity with time, likely below detectable limits, due to the shorter half-lives of these isotopes. The unrealistically high count rates of these simulations should not be of concern since the detector simulations used a very simple geometry. In a real measurement sample, self-shielding will attenuate some of the gamma rays and there will likely be more shielding and distance between the sample and detector. This work is meant to convey the viability of follow-on research.

When comparing the ORIGEN2 burnup simulations to the MCNP burnup simulations, very few differences in the shape of the spectra are discernible for any of the reactor types. Given the fact that ORIGEN2 uses significantly older data, this implies that the assumptions made by the two codes have minimal effect on the generated gamma spectra from the extracted protactinium. The results from the MSR simulations, shown in Appendix E, indicate that the gamma spectra are

similar to those of other reactor types for the first few days of the simulation. However, rather than leaving the protactinium isotopes to decay as in the PWR and CANDU reactors, the MSR periodically extracts the protactinium from the fuel to add to the tank. This allows for all the protactinium isotope quantities to increase before approaching equilibrium (between 100-300 days as shown in Figure 14). If an MSR design uses a batch process where all material in the tank is processed at once and the tank subsequently emptied and allowed to refilled again, the gamma spectra could look substantially different because the protactinium isotopes would not be allowed to reach equilibrium. With MSRs still being designed, it is not known if MSR designs with online fuel processing will implement a continuous or batch approach with the protactinium tank processing. Engaging MSR designers would assist researchers in refining appropriate assumptions regarding continuous versus batch operations.

4. CONCLUSIONS AND FUTURE WORK

Thorium has been suggested as a nuclear fuel alternative and many countries have shown interest in its use. It can be implemented in many traditional reactor designs as well as some yet-to-be built designs. This study focused on one potential proliferation pathway of thorium-fueled nuclear reactors: diversion of ^{233}Pa, which beta decays to become weapons-usable ^{233}U. Certain detection and measurement methods can be used to determine the quantity of ^{233}Pa in the fuel. While many previous studies have identified potential challenges and solutions including highlighting DA and NDA techniques of potential use [20], the work presented here starts to quantify these challenges and solutions. For the protactinium extraction time steps reported in this paper, ^{233}Pa was identified in isolated protactinium mixtures (with respective daughter products). However, more aspects must be considered such as identification limitations within the reactor facility, protactinium isolation methods, evaluation of HKED capabilities, and additional material

quantification for safeguards purposes to name a few. This research assumes a best-case scenario of the protactinium detection. Each isotope was simulated as an unattenuated point source, which does not fully represent the geometry the protactinium material will be in. To better account for real world conditions, one would have to take into consideration self-shielding, attenuation from surrounding shielding, and gamma background created by nearby radioactive materials. Certain phenomena such as photoelectric effect, Compton scattering, and pair production would appear on the gamma spectra. These phenomena, along with gamma background noise, would possibly make the identification of ^{233}Pa more difficult. An additional factor to consider is that as time goes on, extracted ^{233}Pa will continue to decay, diminishing its quantity and making it more difficult to detect. With some reactor designs utilizing online processing, proliferators may then be able to conduct protracted diversions without being detected, allowing for the unmonitored collection of ^{233}Pa and subsequent production of ^{233}U. As nuclear material accountancy technologies continue to develop, other DA and NDA methods can be investigated and evaluated for ^{233}Pa detection and measurement. With results yielded from this study, it can be stated that detecting the presence and quantity of ^{233}Pa within thorium-fueled reactor facilities seems to be an achievable goal. Considering the potential proliferation pathway of thorium-generated ^{233}Pa for the unsafeguarded production of ^{233}U, it would be prudent to monitor the production and quantity of ^{233}Pa in all thorium-fueled reactors, although thorium fueled PWRs and PHWRs are less of a concern because their used fuel cannot be immediately processed as it leaves the reactor core, unlike MSRs. Just as the production of other special fissionable materials are reported, the potential for diversion and misuse of thorium-generated ^{233}Pa exists and should be included in future discussions of these types of advanced reactor designs.

VITA

VICTORIA A. DAVIS

davisv4@vcu.edu

Education

- **Master of Science: Mechanical and Nuclear Engineering (expected May 2022)**

  Virginia Commonwealth University – Richmond, VA

- **Bachelor of Science: Engineering Science (May 2021)**

  Coastal Carolina University – Conway, SC

- **Bachelor of Science: Applied Physics (May 2021)**

  Coastal Carolina University – Conway, SC

Presentations/Conference Papers

- V. Davis, B. Goddard, G.W. Hitt, C. Gariazzo, "Investigation of Potential Protactinium Safeguards Vulnerabilities for Thorium Fuel Cycles," in *2021 INMM & ESARDA Joint Annual Meeting*, Virtual, August 23 – 26 & August 30 – September 1, 2021.
- V. Davis, B. Goddard, G.W. Hitt, C. Gariazzo, "Safeguarding Thorium-Fueled Reactors: Understanding the Impact of Protactinium," in *2021 ANS Winter Meeting and Technology Expo*, Washington, D.C., November 30 – December 3, 2021.
- V. Davis, "Detecting Ionizing Radiation in Space with Memristor Device," in *2021 ANS Student Conference*, Virtual, April 8 – 10, 2021.

REFERENCES

[1] "Nuclear explained," United States Energy Information Administration, April 2021. [Online]. Available: https://www.eia.gov/energyexplained/nuclear/us-nuclear-industry.php.

[2] "Nuclear Power is the Most Reliable Energy Source and It's Not Even Close," United States Office of Nuclear Energy, March 2021. [Online]. Available: https://www.energy.gov/ne/articles/nuclear-power-most-reliable-energy-source-and-its-not-even-close.

[3] International Atomic Energy Agency, "Thorium Fuel Cycle - Potential Benefits and Challenges," IAEA-TECDOC-1450, Vienna, 2005.

[4] International Atomic Energy Agency, "IAEA Safeguards Glossary: 2001 Edition," 2001.

[5] "Thorium," World Nuclear Association, 2020. [Online]. Available: https://world-nuclear.org/information-library/current-and-future-generation/thorium.aspx.

[6] International Atomic Energy Agency, "Impact of extended burnup on the nuclear fuel cycle," IAEA, Vienna, 1991.

[7] "What is uranium? how does it work?," World Nuclear Association, 2020. [Online]. Available: https://world-nuclear.org/information-library/nuclear-fuel-cycle/introduction/what-is-uranium-how-does-it-work.aspx#:~:text=In%20a%20nuclear%20reactor%20the,drive%20a%20generator%2C%20producing%20electricity.

[8] E. Boechler, J. Hanania, K. Stenhouse, L. V. Suarez and J. Donev, "Energy Education - CANDU reactor," October 2021. [Online]. Available: https://energyeducation.ca/encyclopedia/CANDU_reactor.

[9] B. Rouben, "CANDU Fuel-Management Course," Atomic Energy of Canada Ltd., https://canteach.candu.org/content%20library/20031101.pdf, 2003.

[10] D. N. Kovacic, L. G. Worrall, A. Worral, G. F. Flanagan, D. E. Holcomb, R. Bari, L. Cheng, D. Farley and M. Sternat, "Safeguards Challenges for Molten Salt Reactors," in *59th Annual Meeting of the Institute of Nuclear Materials Management*, Baltimore, Maryland, July 22-26, 2018.

[11] "The IMSR® plant uses proven molten salt reactor technology with patented enhancements for commercial-scale thermal and electrical energy generation.," Terrestrial Energy Inc., 2022. [Online]. Available: https://www.terrestrialenergy.com/technology/molten-salt-reactor/.

[12] "Molten Salt Reactors," World Nuclear Association, May 2021. [Online]. Available: https://world-nuclear.org/information-library/current-and-future-generation/molten-salt-reactors.aspx.

[13] M. M. Waldrop, "Nuclear Technology Abandoned Decades Ago Might Give Us Safer, Smaller Reactors," 26 February 2019. [Online]. Available: https://www.discovermagazine.com/environment/nuclear-technology-abandoned-decades-ago-might-give-us-safer-smaller-reactors. [Accessed October 2021].

[14] International Atomic Energy Agency, "Safeguards Techniques and Equipment: 2011 Edition," 2011.

[15] International Atomic Energy Agency, "Statute," 1989.

[16] E. C. Uribe, "Protactinium Presents a Challenge for Safeguarding Thorium Reactors," Sandia National Laboratory, Livermore, 2018.

[17] International Atomic Energy Agency, "International Safeguards in the Design of Nuclear Reactors," 2014.

[18] A. Worral, J. W. Bae, B. R. Betzler, S. Greenwood and L. G. Worrall, "Molten Salt Reactor Safeguards: The Necessity of Advanced Modeling and Simulation to Inform on Fundamental Signatures," Oak Ridge National Laboratory, 2019.

[19] A. Worrall, B. Betzler, G. Flanagan, D. Holcomb, J. Hu, D. Kovacic, L. Qualls and L. Worrall, "Molten Salt Reactors and Associated Safeguards Challenges and Opportunities," in *IAEA Symposium on International Safeguards*, Vienna, Austria, 2018.

[20] A. Swift, K. Hogue, T. Folk and J. Cooley, "Safeguards Technical Objectives for Thorium Molten Salt Reactor Fuel Cycles," in *61st Annual Meeting of the Institute of Nuclear Materials Management*, 2020.

[21] C. Lloyd and B. Goddard, "Impact of Gamma Ray Emissions of Materials Containing 232U on Safety, Security, and Safeguards," *Nuclear Engineering and Design,* Vols. 370, 110905, 2020.

[22] C. Lloyd, B. Goddard and R. Witherspoon, "The effects of U-232 on Enrichment and Material Attractiveness over Time," *Nuclear Engineering and Design,* Vols. 352, 110175, 2019.

[23] S. Boulyga, S. Konegger-Kappel, S. Richter and L. Sangely, "Mass spectrometric analysis for nuclear safeguards," *J. Anal. At. Spectrom.,* vol. 30, no. 7, pp. 1469-1489, 2015.

[24] D. Suzuki, F. Esaka, Y. Miyamoto and M. Magara, "Direct isotope ratio analysis of individual uranium-plutonium mixed particles with various U/Pu ratios by thermal ionization mass spectrometry," *Applied Radiation and Isotopes,* vol. 96, pp. 52-56, 2014.

[25] G. R. Eppich, Z. Macsik, R. Katona, S. Konegger-Kappel, G. Stadelmann, A. Kopf, B. Varga and S. Boulyga, "Plutonium assay and isotopic composition measurements in nuclear safeguards samples

by inductively coupled plasma mass spectrometry," *J. Anal. At. Spectrom.,* vol. 34, no. 6, pp. 1154-1165, 2019.

[26] A. Quemet, A. Ruas, V. Dalier and C. Rivier, "Development and comparison of high accuracy thermal ionization mass spectrometry methods for uranium isotope ratios determination in nuclear fuel," *International Jounral of Mass Spectrometry,* vol. 438, pp. 166-174, 2019.

[27] F. Wang, Y. Zhang, Y.-g. Zhao, D.-f. Guo, S.-k. Xie, J. Tan, J.-y. Li and J. Lu, "Application of laser ionization mass spectrometry for measurement of uranium isotope ratio in nuclear forensics and nuclear safeguards," *Meas. Sci. Technol.,* vol. 29, no. 9, 2018.

[28] J. B. Coble, S. E. Skutnik, S. N. Gilliam and M. P. Cooper, "Review of Candidate Techniques for Material Accountancy Measurements in Electrochemical Separations Facilities," *Nuclear Technology,* vol. 206, no. 12, pp. 1803-1826, 2020.

[29] Z. Varga, M. Krachler, A. Nicholl, M. Ernstberger, T. Wiss, M. Wallenius and K. Mayer, "Accurate measurement of uranium isotope ratios in solid samples by laser ablation multi-collector inductively coupled plasma mass spectrometry," *J. Anal. At. Spectrom.,* vol. 33, no. 6, pp. 1076-1080, 2018.

[30] D. Harvey, "Chapter 8: Gravimetric Methods," in *Analytical Chemistry 2.0*, 2011, pp. 355-409.

[31] R. D. Braun, "Chemical analysis," in *Encyclopedia Britannica*, 2016.

[32] "Precipitation Gravimetry," LibreTexts, September 2021. [Online]. Available: https://chem.libretexts.org/Bookshelves/Analytical_Chemistry/Analytical_Chemistry_2.1_(Harvey)/08%3A_Gravimetric_Methods/8.02%3A_Precipitation_Gravimetry#:~:text=In%20precipitation%20gravimetry%20an%20insoluble,solution%20that%20contains%20our%20analyte..

[33] J. E. Stewart, "Principles of Total Neutron Counting," in *Passive Nondestructive Assay of Nuclear Materials*, 1991, pp. 407-434.

[34] D. DeSimone, A. Favalli, D. MacArthur, C. Moss and J. Thron, "Review of Active Interrogation Techniques and Considerations for Their Use behind an Information Barrier," Los Alamos National Laboratory, Los Alamos, New Mexico, LA-UR-10-06958, 2010.

[35] "Nuclear Data Center at KAERI," [Online]. Available: https://atom.kaeri.re.kr/.

[36] A. Gavron and S. T. Hsue, "KED/KXRF Hybrid Densitometer," Los Alamos National Laboratory, Los Alamos, 1996.

[37] *International Nuclear Safeguards Solutions,* Canberra, 2017.

[38] A. N. William and S. Phongikaroon, "Laser-Induced Breakdown Spectroscopy (LIBS) in a Novel Molten Salt Aerosol System," *Applied Spectroscopy,* vol. 71, no. 4, pp. 744-749, 2017.

[39] A. Williams and S. Phongikaroon, "Laser-Induced Breakdown Spectroscopy (LIBS) Measurement of Uranium in Molten Salt," *Applied Spectroscopy,* vol. 72(7), pp. 1029-1039, 2018.

[40] D. K. Hauck, D. S. Bracken, D. W. MacArthur, P. A. Santi and J. Thron, "Feasibility study on using fast calorimetry technique to measure a mass attribute as part of a treaty verification regime," Los Alamos National Laboratory, Los Alamos, New Mexico, LA-UR-10-03786, 2010.

[41] S. Croft, S. Phillips, L. G. Evans, J. Guerault, G. Jossens, L. Passelegue and C. Mathonat, "Nuclear Calorimetry - Dispelling the Myths," in *WM2010 Conference*, Phoenix, Arizona, March 7-11, 2010.

[42] T. L. Cremers and T. E. Sampson, "Calorimetry of low mass Pu239 items," 2010 New Brunswick Laboratory Measurement Evaluation Program Meeting, LA-UR-10-03477, 2010.

[43] C. R. Rudy, D. S. Bracken, M. K. Smith and M. J. Schanfein, "Calorimetry of TRU Waste Materials," in *Spectrum 2000 International Conference on Nuclear and Hazardous Waste Management*, Chattanooga, 2000.

[44] L. W. Campbell, L. E. Smith and A. C. Misner, "High-Energy Delayed Gamma Spectroscopy for Spent Nuclear Fuel Assay," *IEEE Transactions on Nuclear Science,* vol. 58, no. 1, pp. 231-240, 2011.

[45] I. C. Gauld and M. W. Francis, "Investigation of Passive Gamma Spectroscopy to Verify Spent Nuclear Fuel Content," in *51st Annual Meeting of the Institute of Nuclear Materials Management*, Baltimore, Maryland, 2010.

[46] C. J. Werner, "MCNP6.2 Release Notes," Los Alamos National Laboratory, 2018.

[47] L. Hiller, T. Gosnell, J. Gronberg and D. Wright, "RadSrc Library and Application Manual," Lawrence Livermore National Laboratory, 2013.

[48] A. G. Croff, "User's manual for the ORIGEN2 computer code," Oak Ridge National Laboratory, 1980.

[49] "RSICC Computer Code CCC-371," Oak Ridge NationalLaboratory, [Online]. Available: https://rsicc.ornl.gov/codes/ccc/ccc3/ccc-371.html. [Accessed December 2021].

[50] Oak Ridge National Laboratory, "SCALE Code System," United States Department of Energy, 2018.

[51] "SCALE/TRITON Primer: A Primer for Light Water Reactor Lattice Physics Calculations," United States Nuclear Regulatory Commission, 2011.

[52] H. R. Trellue, C. G. Bathke and P. Sadasivan, "Neutronics and material attractiveness for PWR thorium systems using monte carlo techniques," *Progress in Nuclear Energy,* vol. 53, no. 6, pp. 698-707, 2011.

[53] P. G. Boczar, G. R. Dyck, P. S. W. Chan and D. B. Buss, "Recent advances in thorium fuel cycles for CANDU reactors," in *Thorium fuel utilization: Options and trends*, 2002.

[54] O. Ashraf, A. Rykhlevskii, G. V. Tikhomirov and K. D. Huff, "Whole core analysis of the single-fluid double-zone thorium molten salt reactor (SD-TMSR)," *Annals of Nuclear Energy,* vol. 137, 2020.

[55] J. Kang and F. Hippel, "U-232 and the Proliferation Resistance of U-233 in Spent Fuel," *Science & Global Security,* vol. 9, pp. 1-32, 2001.

APPENDIX A

Gamma spectra for ^{232}Pa, ^{233}Pa, and ^{234}Pa.

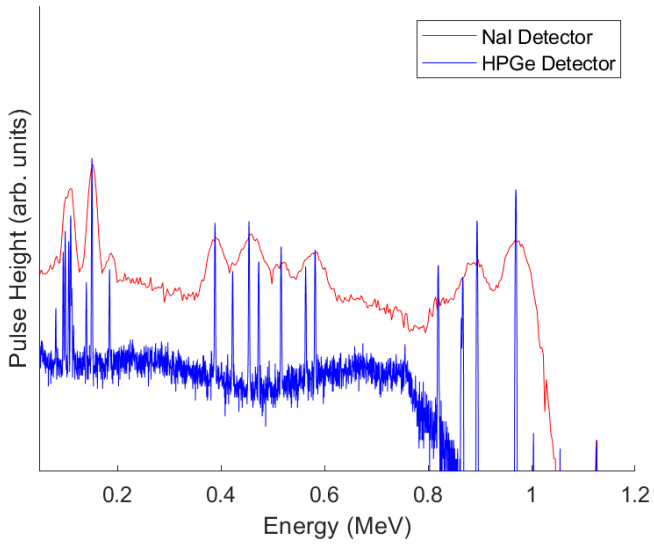

Figure A1: ^{232}Pa gamma spectrum.

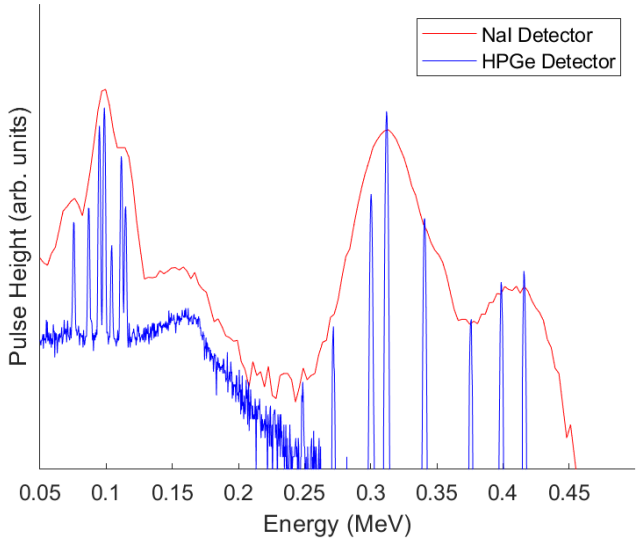

Figure A2: ^{233}Pa gamma spectrum.

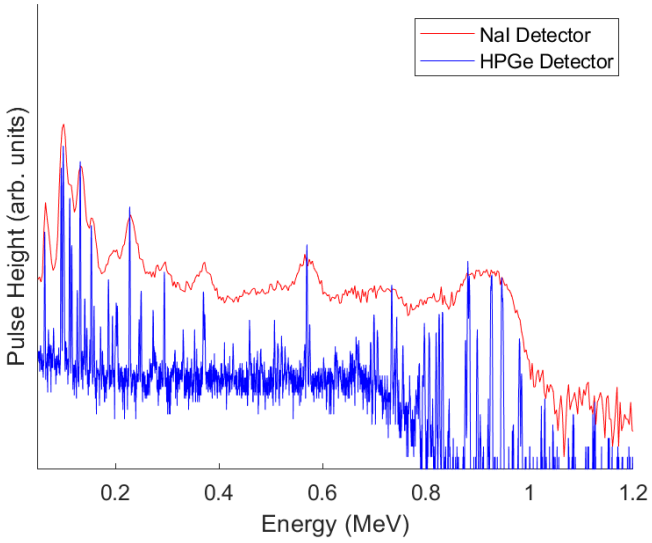

Figure A3: ^{234}Pa gamma spectrum.

APPENDIX B

ORIGEN2 output for Pa and U.

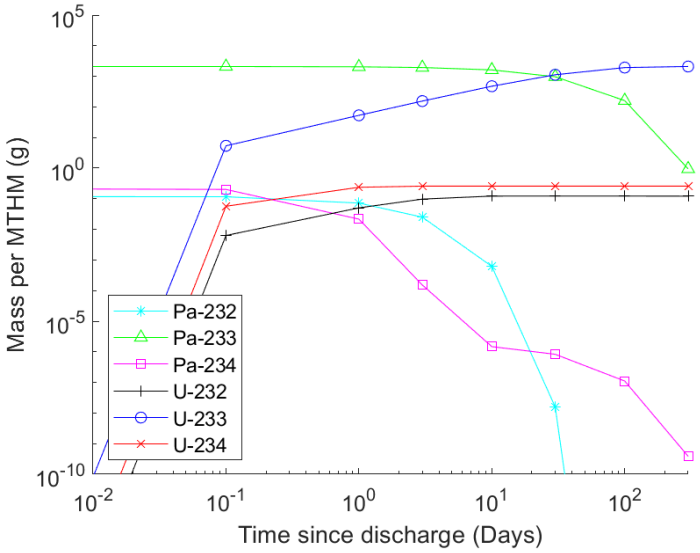

Figure B1: Relative abundance of isotopes for PWRUS.

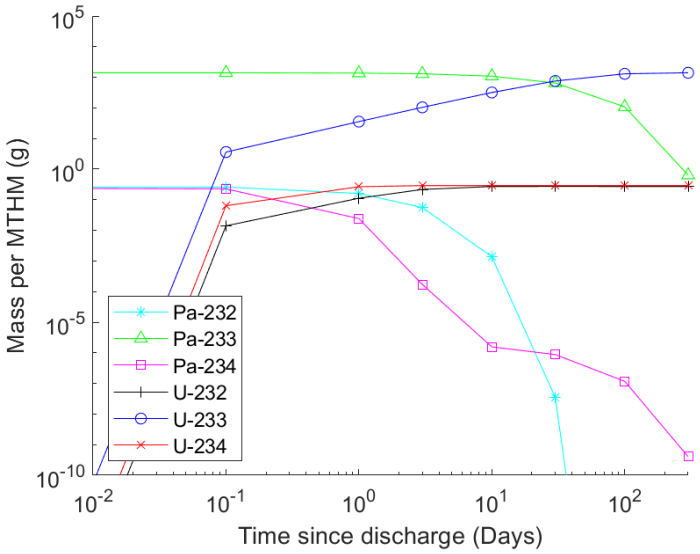

Figure B2: Relative abundance of isotopes for PWRD5D35.

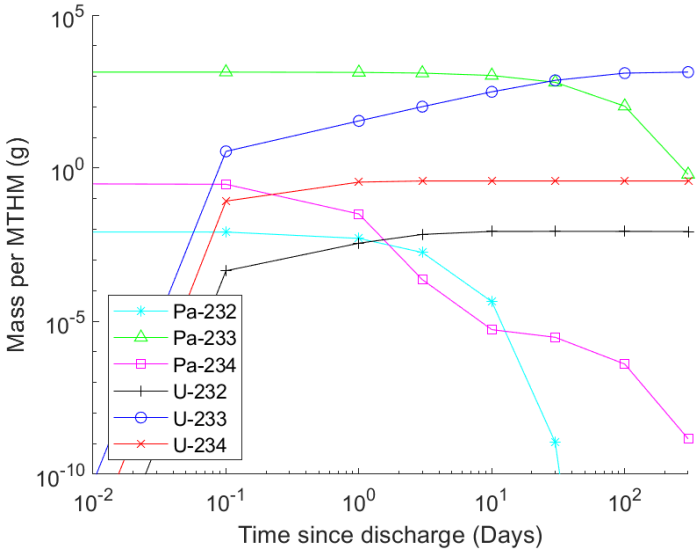

Figure B3: Relative abundance of isotopes for CANDUNAU.

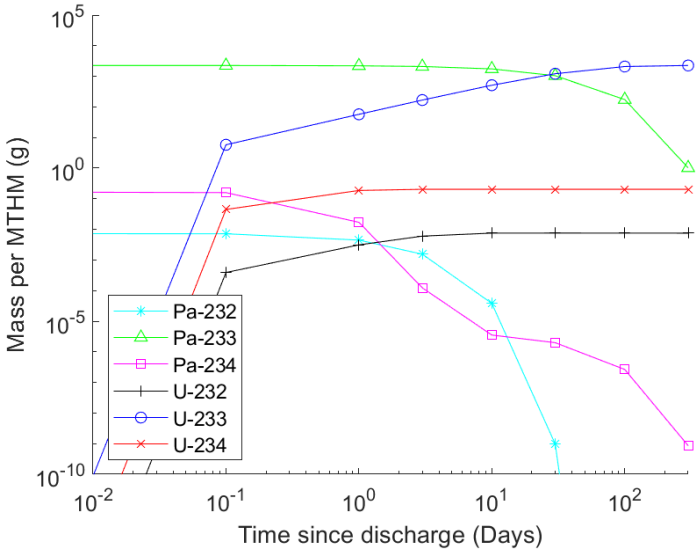

Figure B4: Relative abundance of isotopes for CANDUSEU.

APPENDIX C

Gamma spectra for separated protactinium mixture for ORIGEN2 burnup simulations.

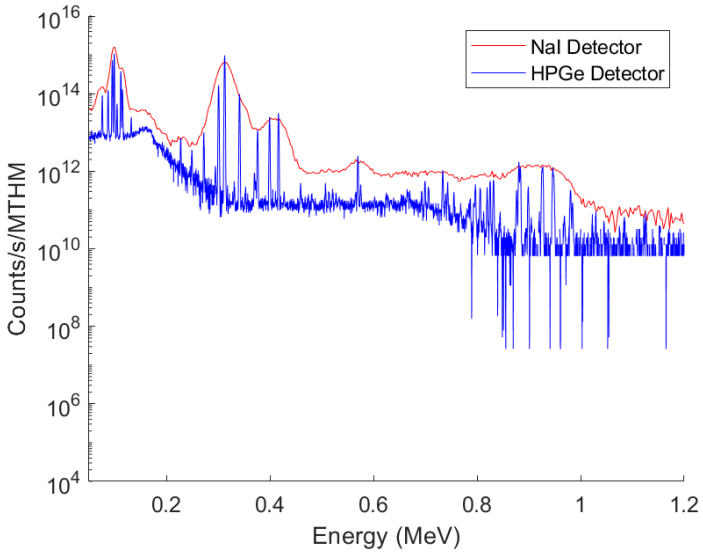

Figure C1: Gamma spectrum for PWRUS at 0 days.

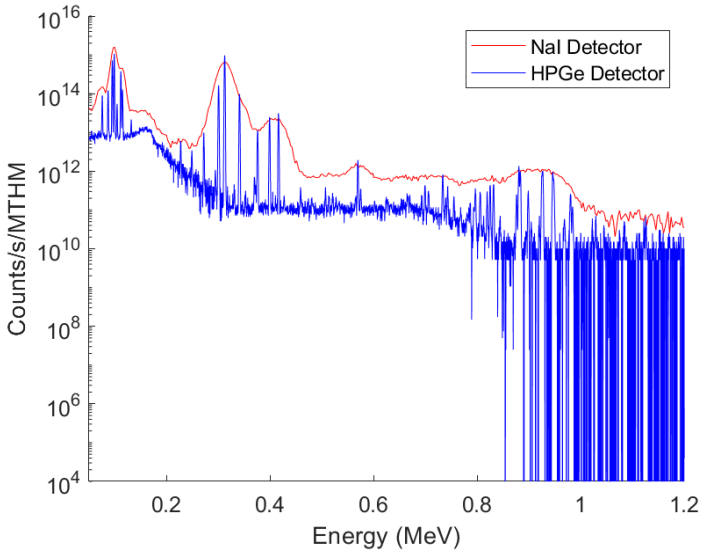

Figure C2: Gamma spectrum for PWRUS at 0.1 days.

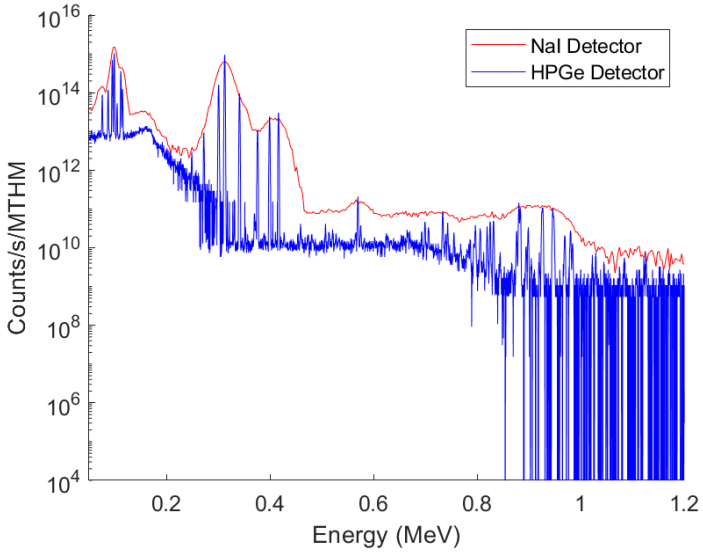

Figure C3: Gamma spectrum for PWRUS at 1 day.

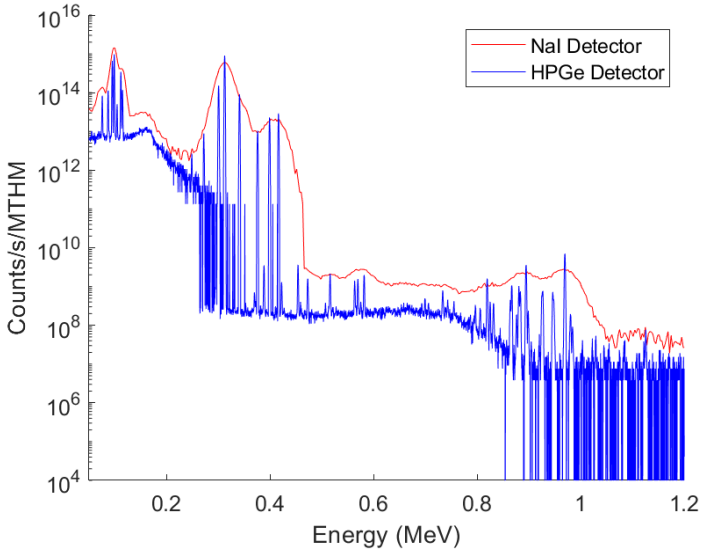

Figure C4: Gamma spectrum for PWRUS at 3 days.

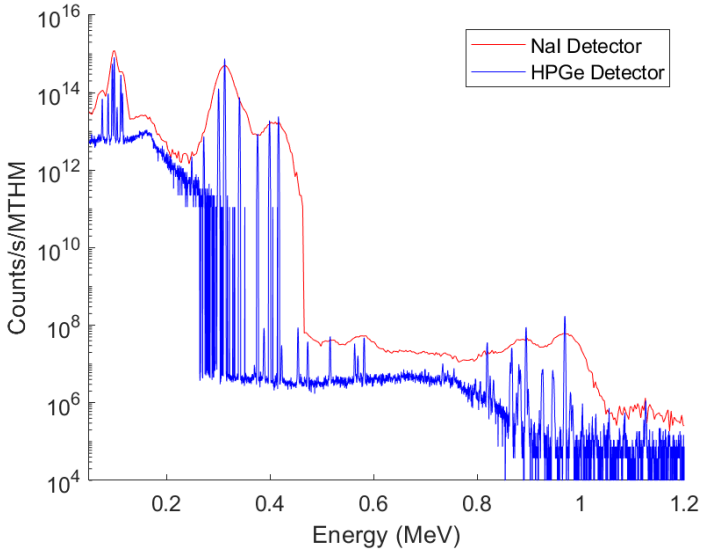

Figure C5: Gamma spectrum for PWRUS at 10 days.

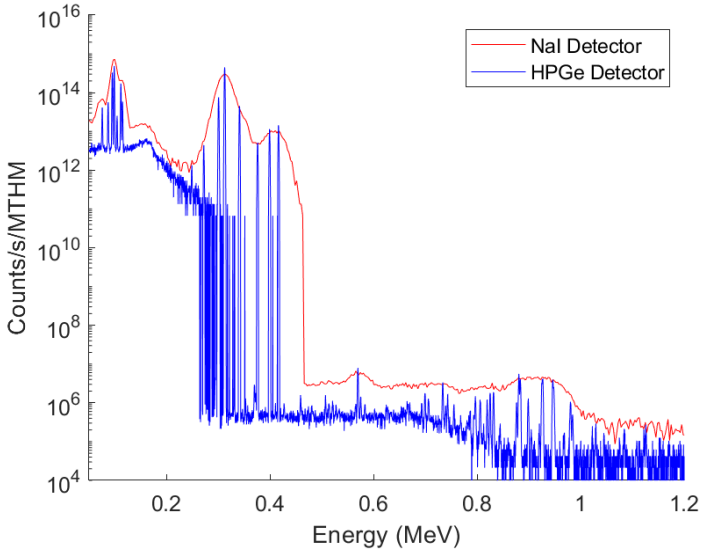

Figure C6: Gamma spectrum for PWRUS at 30 days.

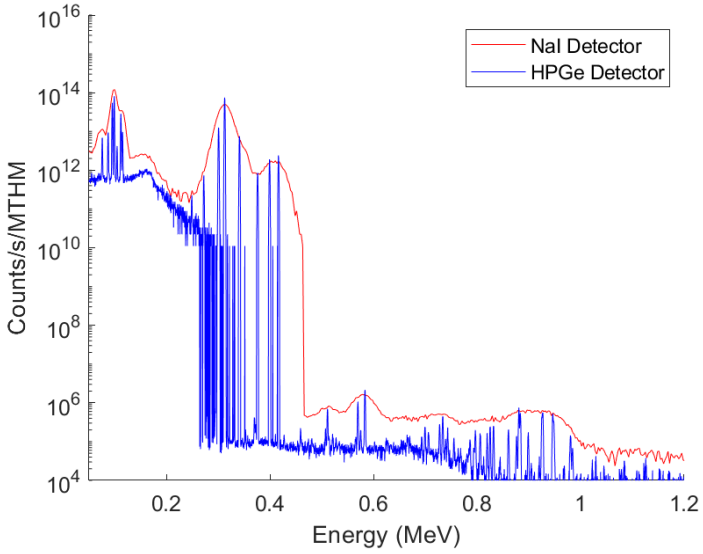

Figure C7: Gamma spectrum for PWRUS at 100 days.

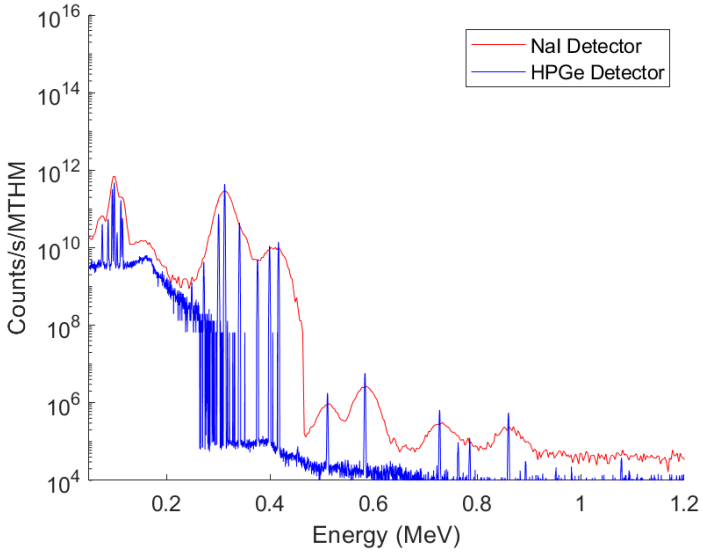

Figure C8: Gamma spectrum for PWRUS at 300 days.

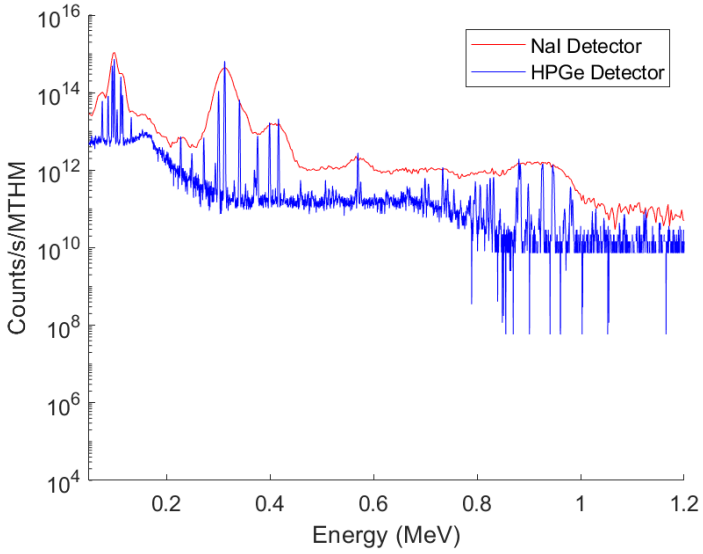

Figure C9: Gamma spectrum for PWRD5D35 at 0 days.

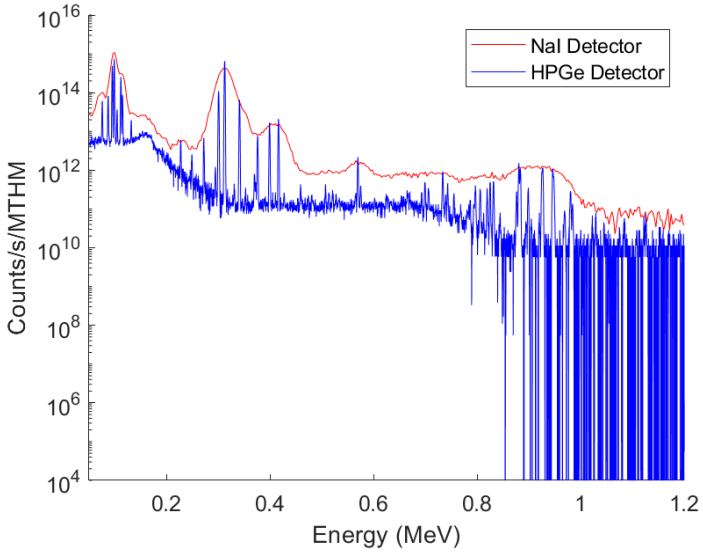

Figure C10: Gamma spectrum for PWRD5D35 at 0.1 days.

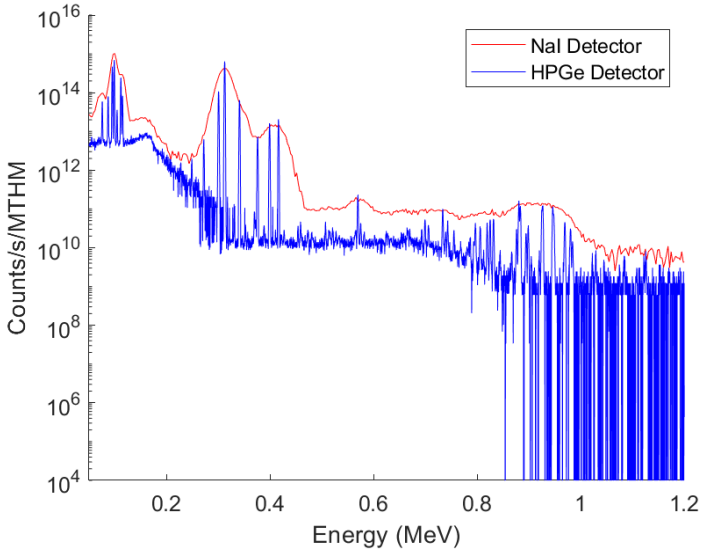

Figure C11: Gamma spectrum for PWRD5D35 at 1 day.

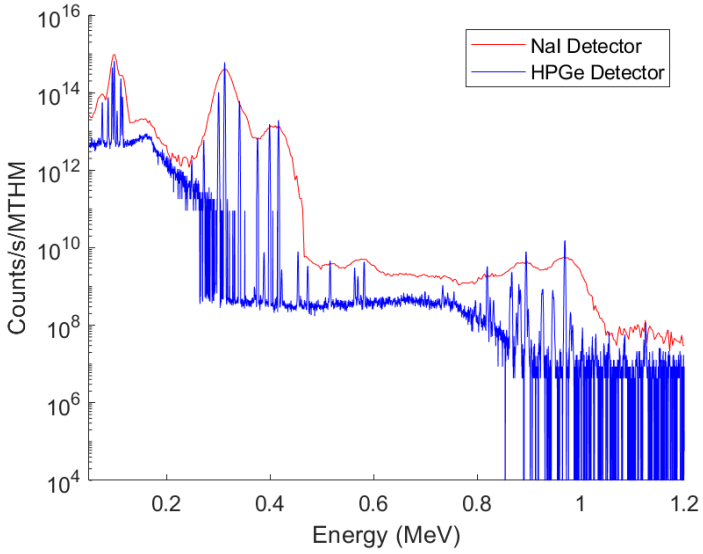

Figure C12: Gamma spectrum for PWRD5D35 at 3 days.

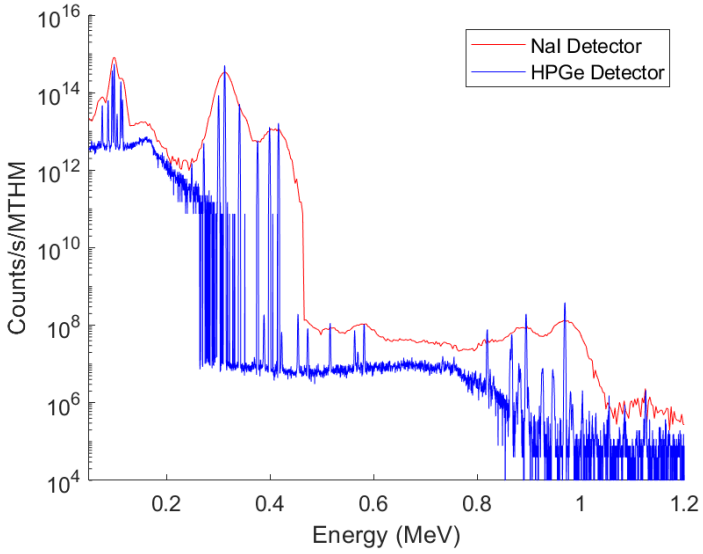

Figure C13: Gamma spectrum for PWRD5D35 at 10 days.

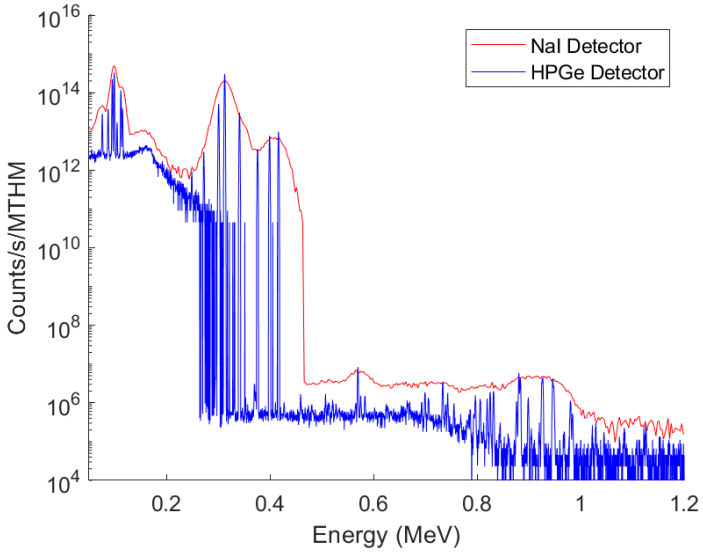

Figure C14: Gamma spectrum for PWRD5D35 at 30 days.

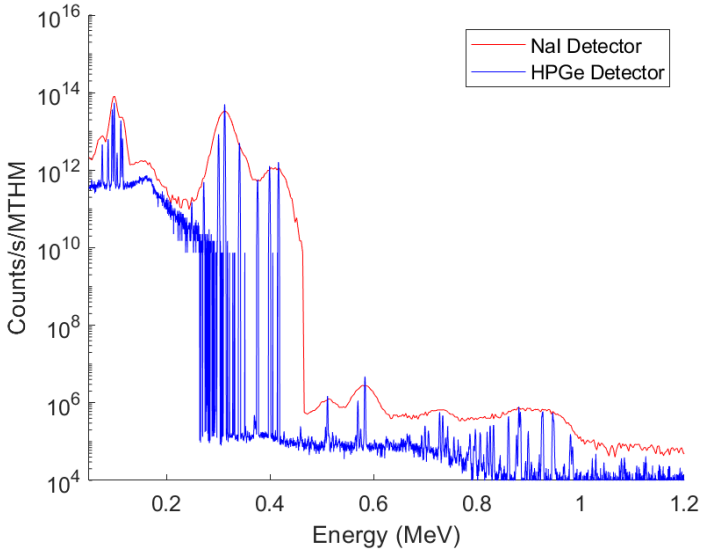

Figure C15: Gamma spectrum for PWRD5D35 at 100 days.

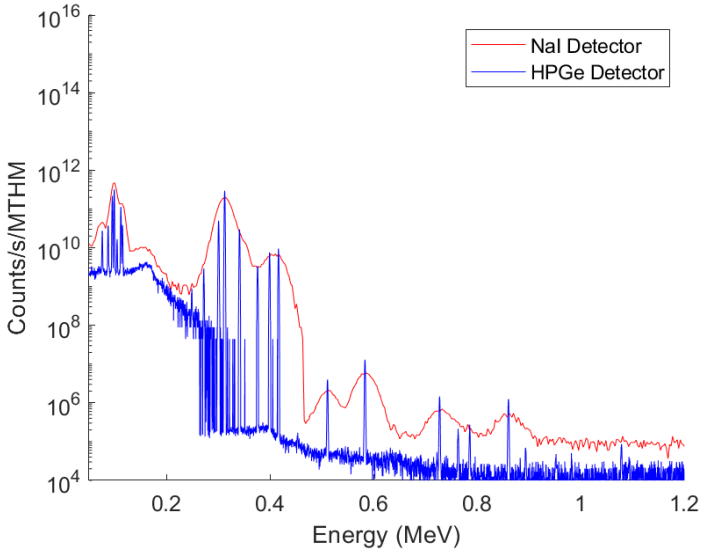

Figure C16: Gamma spectrum for PWRD5D35 at 300 days.

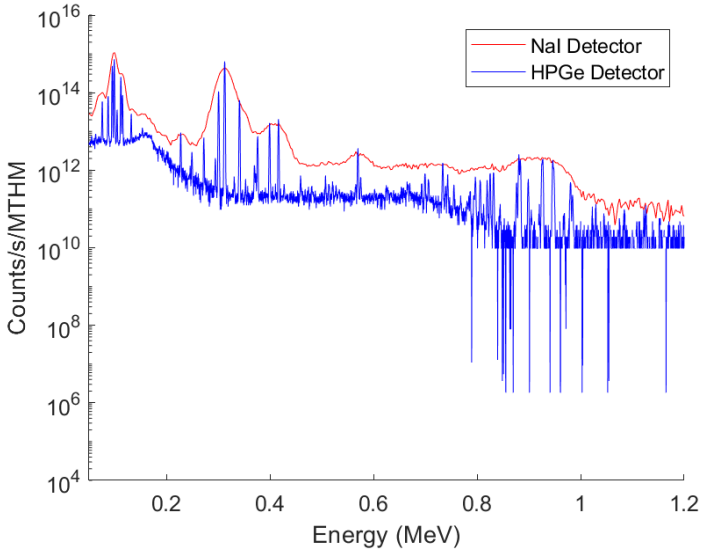

Figure C17: Gamma spectrum for CANDUNAU at 0 days.

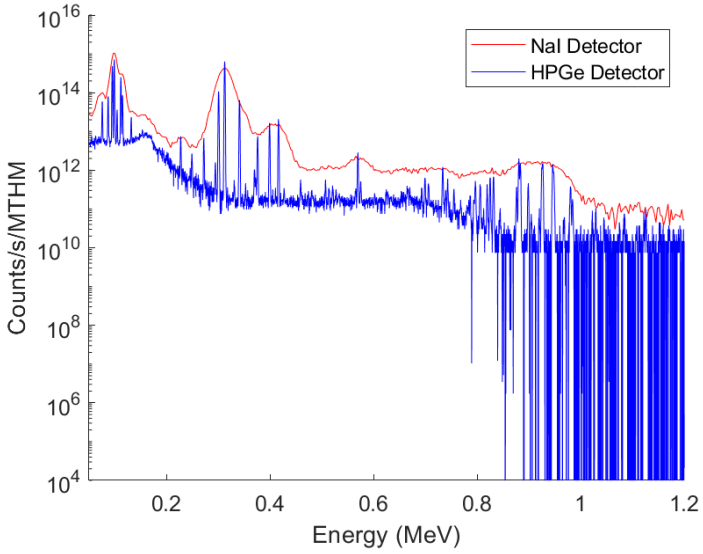

Figure C18: Gamma spectrum for CANDUNAU at 0.1 days.

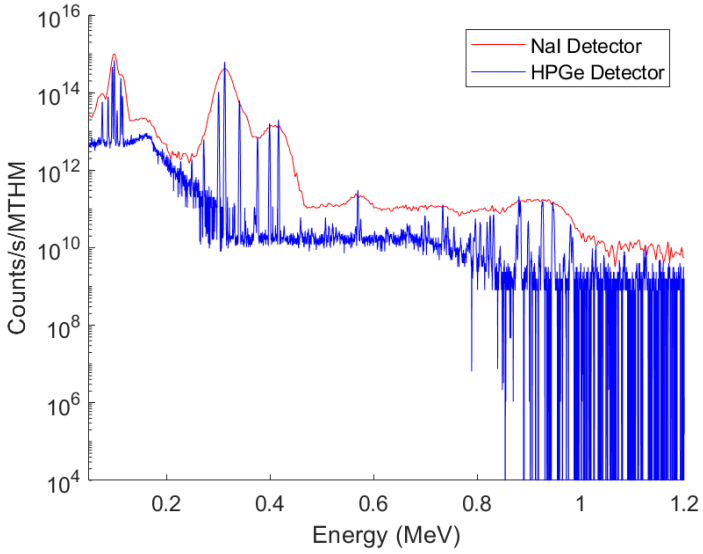

Figure C19: Gamma spectrum for CANDUNAU at 1 day.

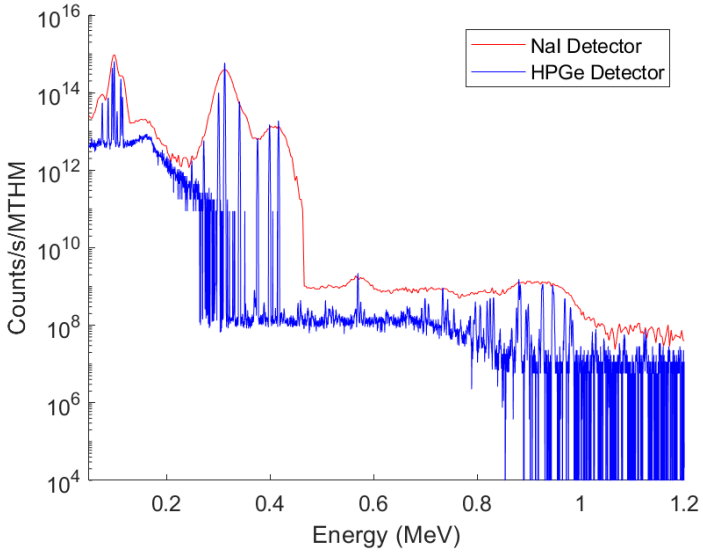

Figure C20: Gamma spectrum for CANDUNAU at 3 days.

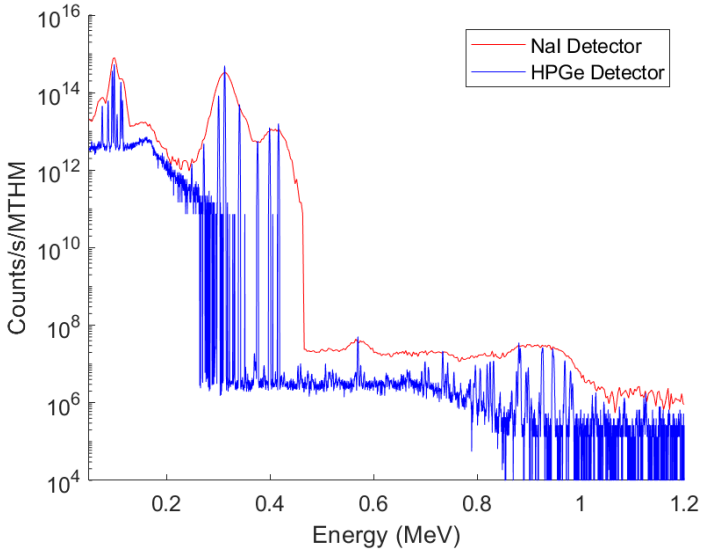

Figure C21: Gamma spectrum for CANDUNAU at 10 days.

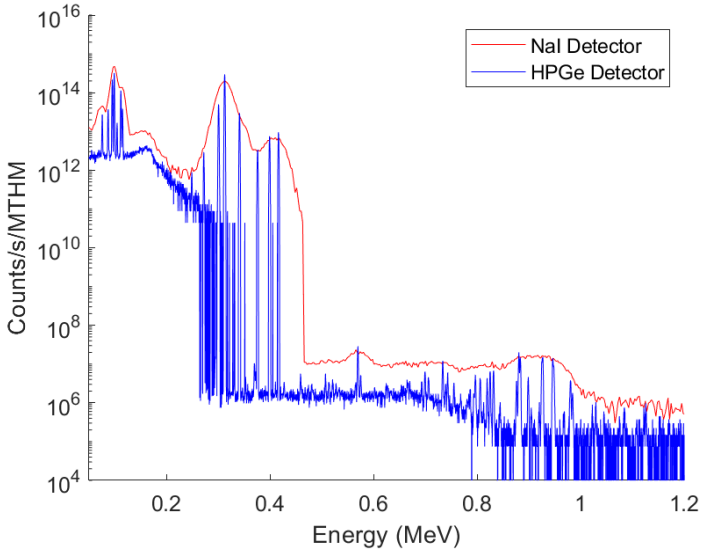

Figure C22: Gamma spectrum for CANDUNAU at 30 days.

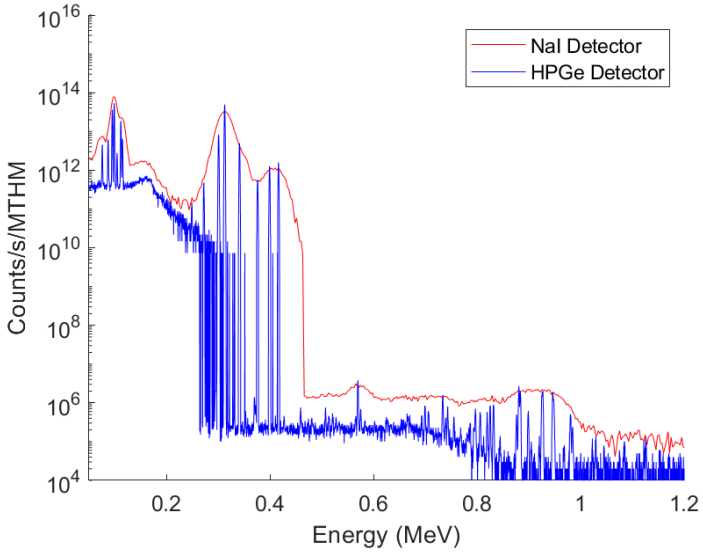

Figure C23: Gamma spectrum for CANDUNAU at 100 days.

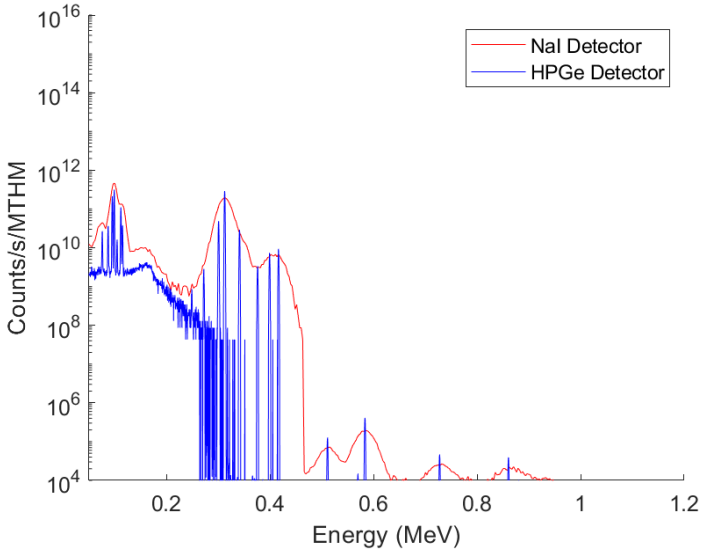

Figure C24: Gamma spectrum for CANDUNAU at 300 days.

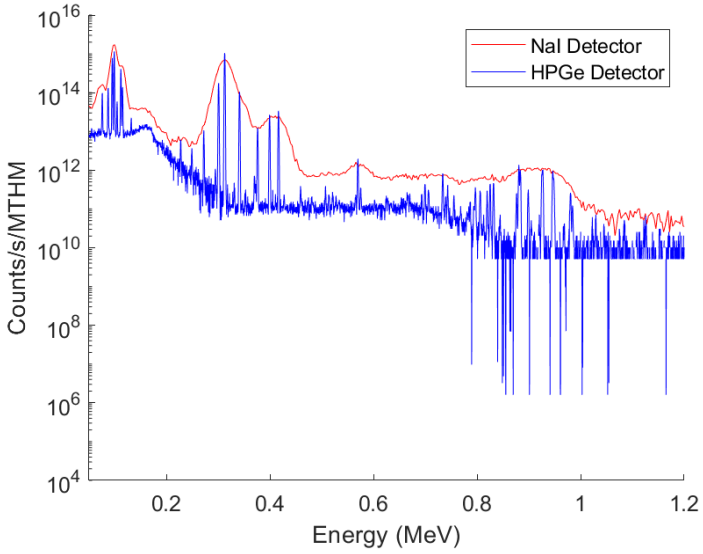

Figure C25: Gamma spectrum for CANDUSEU at 0 days.

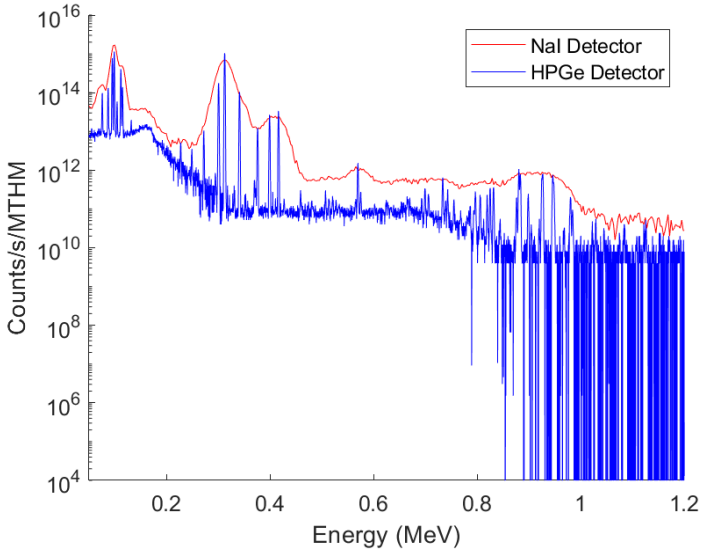

Figure C26: Gamma spectrum for CANDUSEU at 0.1 days.

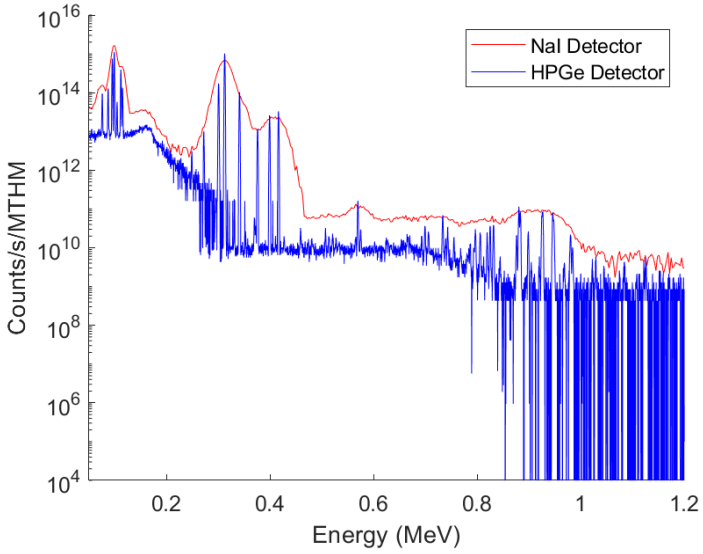

Figure C27: Gamma spectrum for CANDUSEU at 1 day.

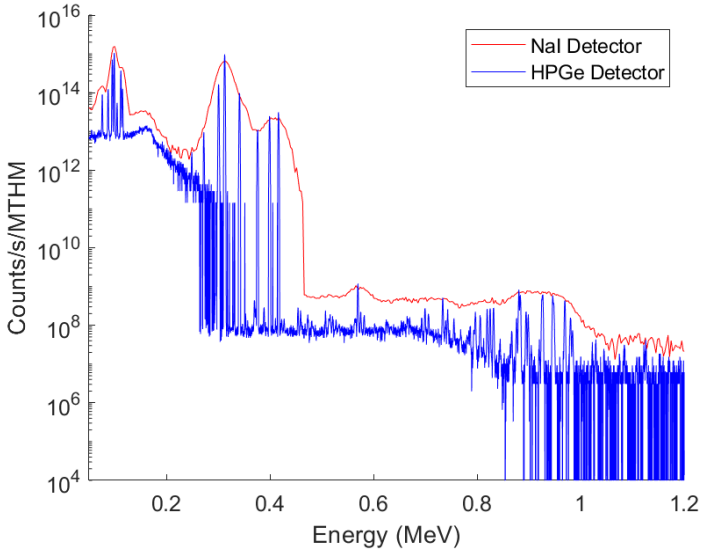

Figure C28: Gamma spectrum for CANDUSEU at 3 days.

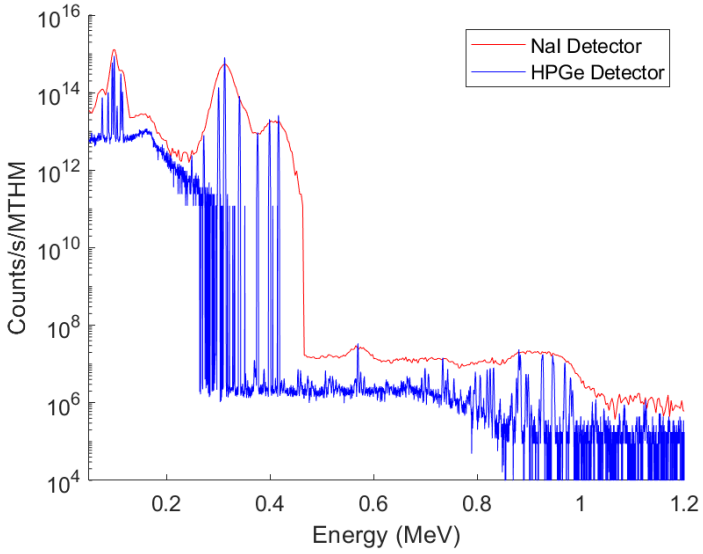

Figure C29: Gamma spectrum for CANDUSEU at 10 days.

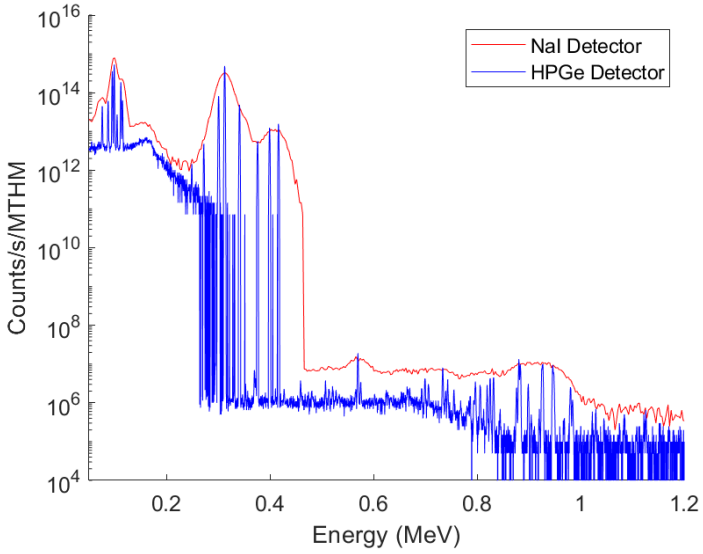

Figure C30: Gamma spectrum for CANDUSEU at 30 days.

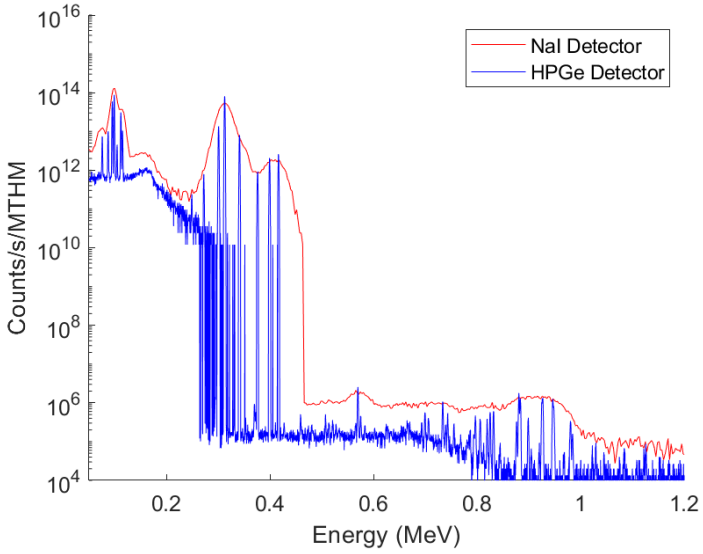

Figure C31: Gamma spectrum for CANDUSEU at 100 days.

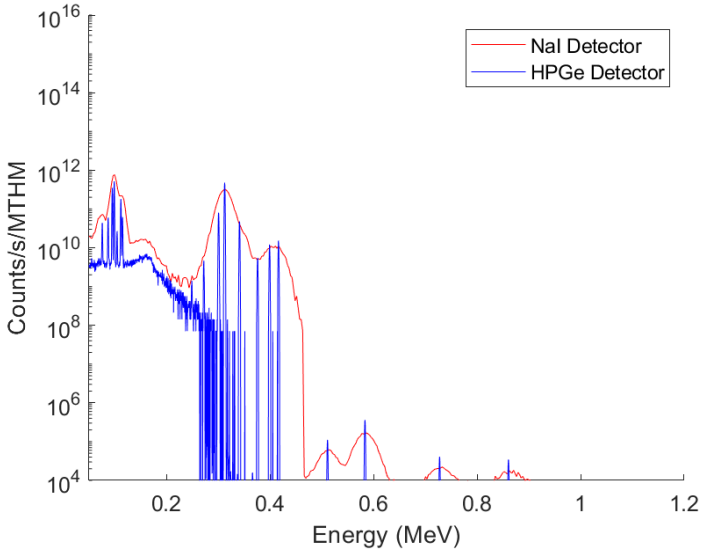

Figure C32: Gamma spectrum for CANDUSEU at 300 days.

APPENDIX D

Gamma spectra for separated protactinium mixture for MCNP burnup simulations.

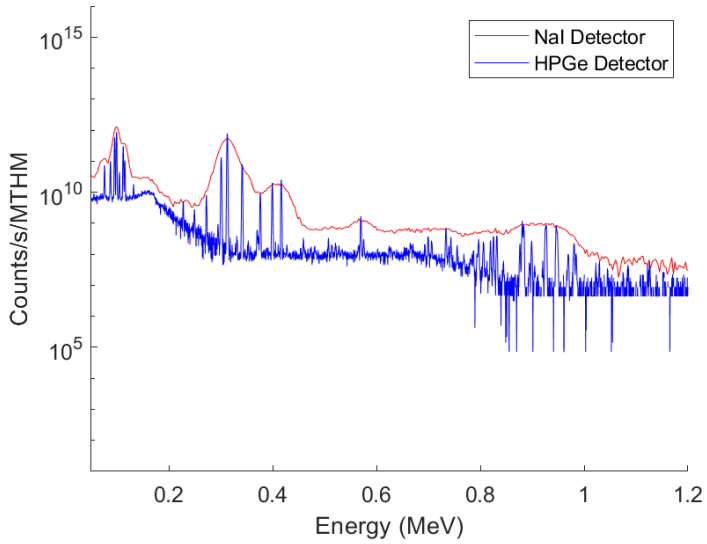

Figure D1: Gamma spectrum for PWR at 0 days.

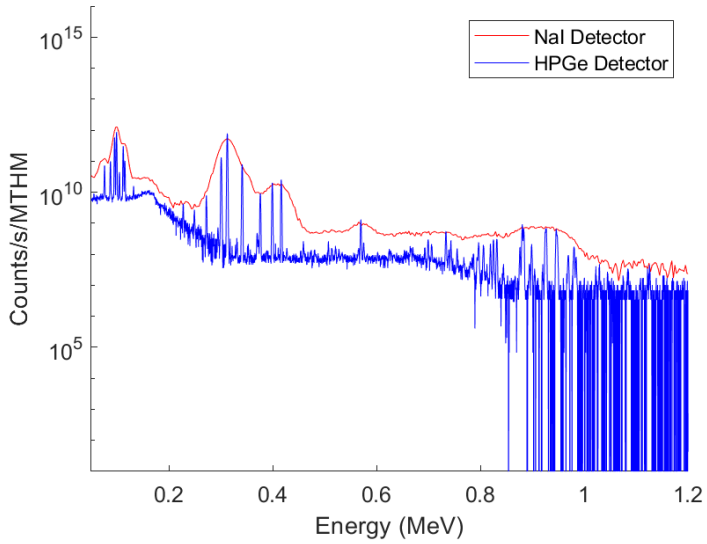

Figure D2: Gamma spectrum for PWR at 0.1 days.

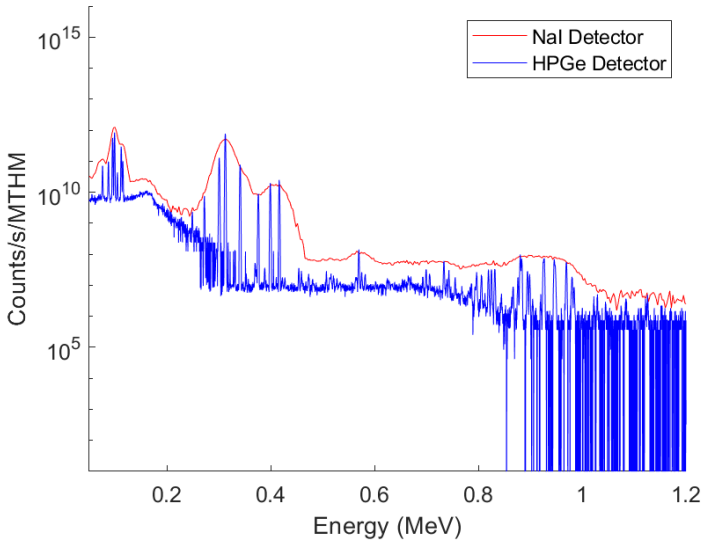

Figure D3: Gamma spectrum for PWR at 1 day.

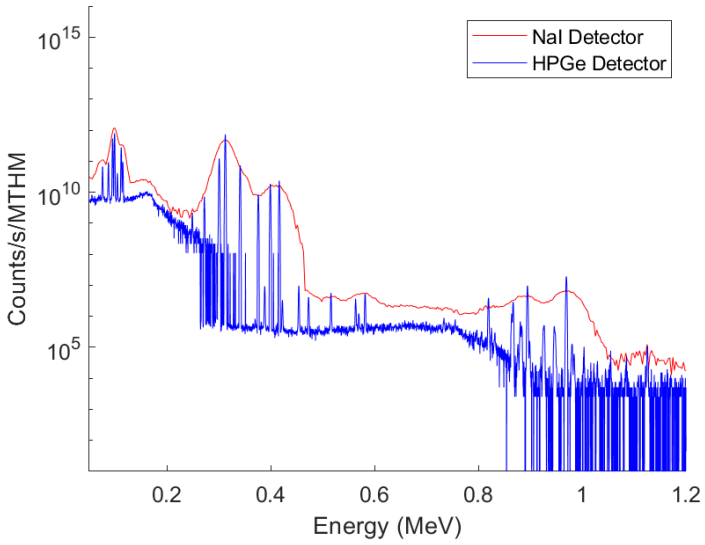

Figure D4: Gamma spectrum for PWR at 3 days.

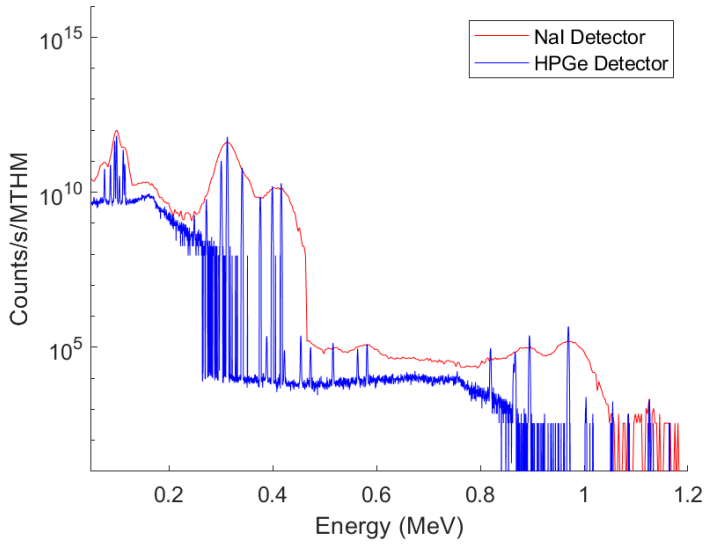

Figure D5: Gamma spectrum for PWR at 10 days.

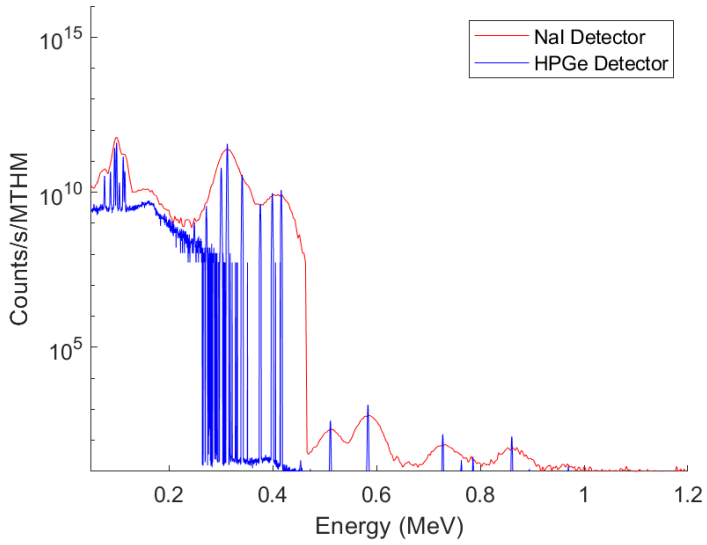

Figure D6: Gamma spectrum for PWR at 30 days.

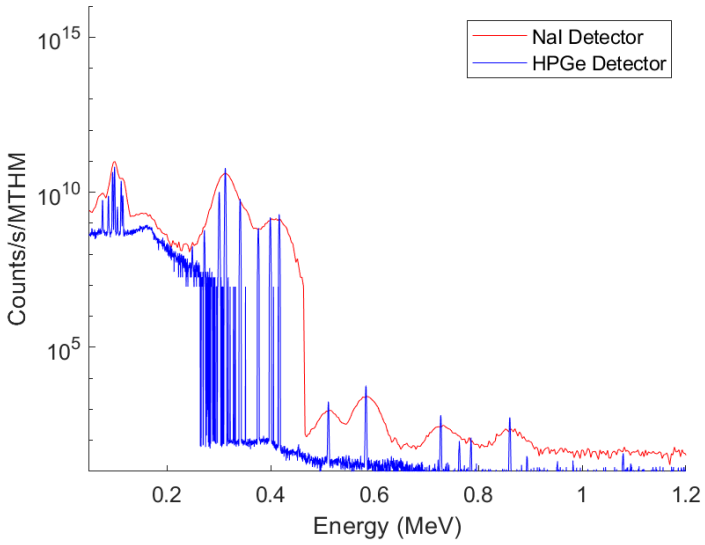

Figure D7: Gamma spectrum for PWR at 100 days.

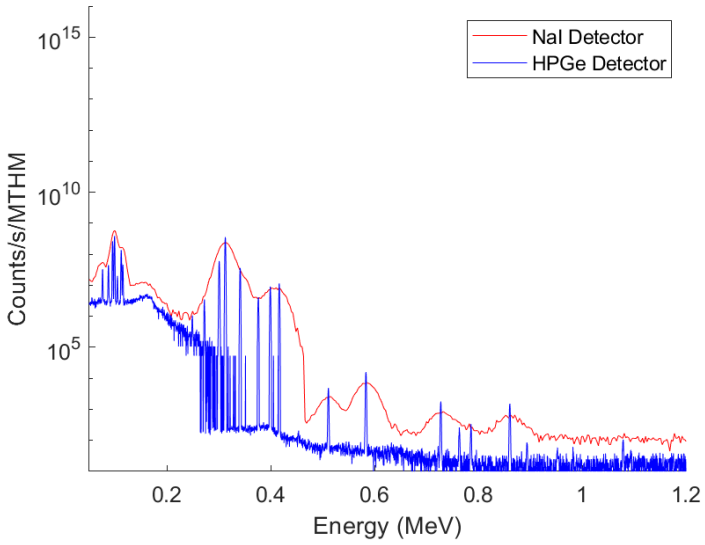

Figure D8: Gamma spectrum for PWR at 300 days.

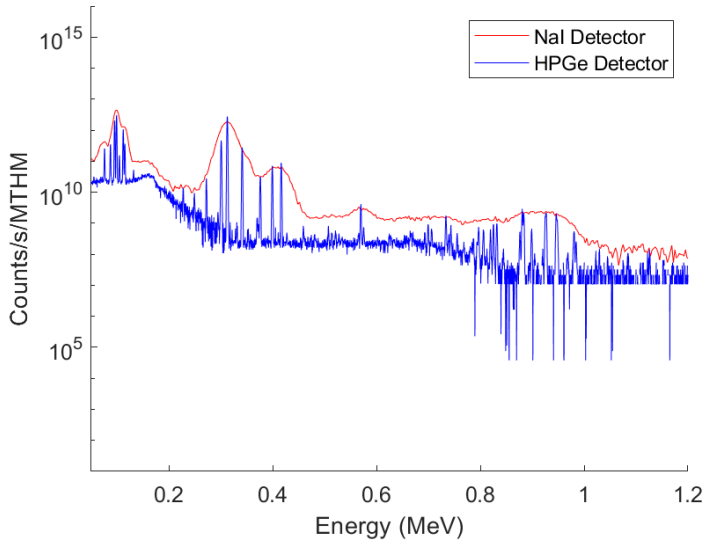

Figure D9: Gamma spectrum for CANDU (0.711% enriched uranium) at 0 days.

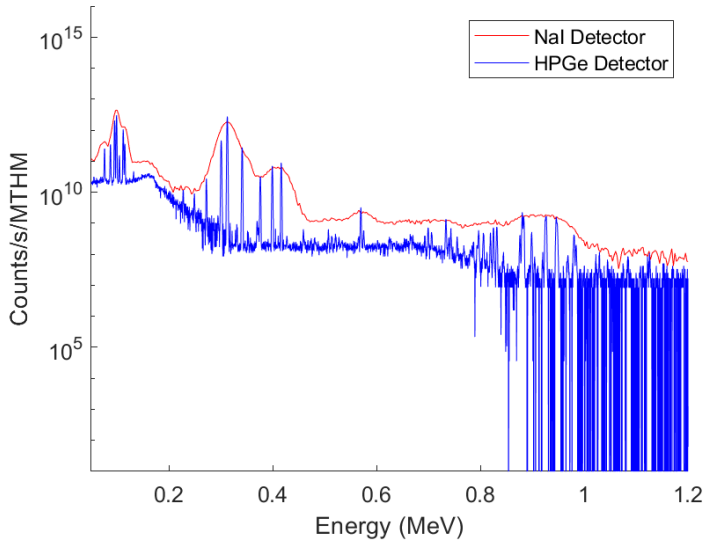

Figure D10: Gamma spectrum for CANDU (0.711% enriched uranium) at 0.1 days.

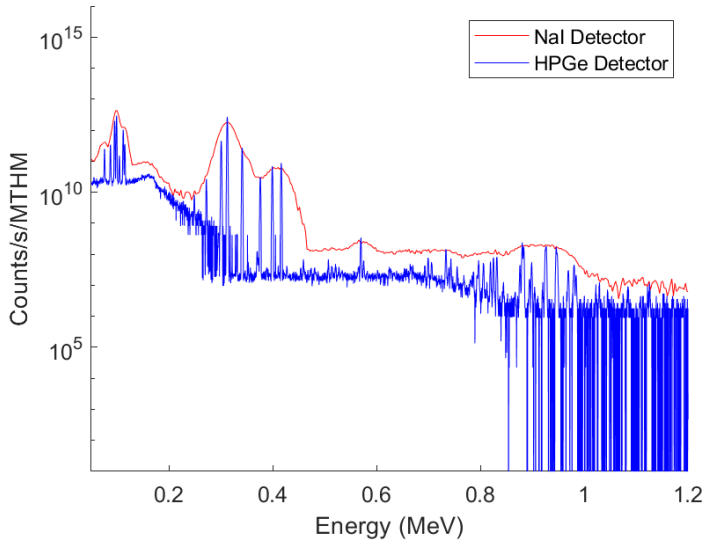

Figure D11: Gamma spectrum for CANDU (0.711% enriched uranium) at 1 day.

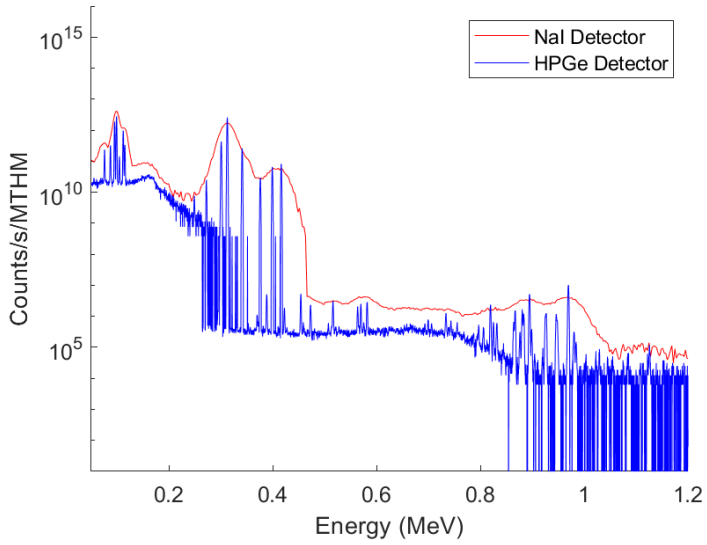

Figure D12: Gamma spectrum for CANDU (0.711% enriched uranium) at 3 days.

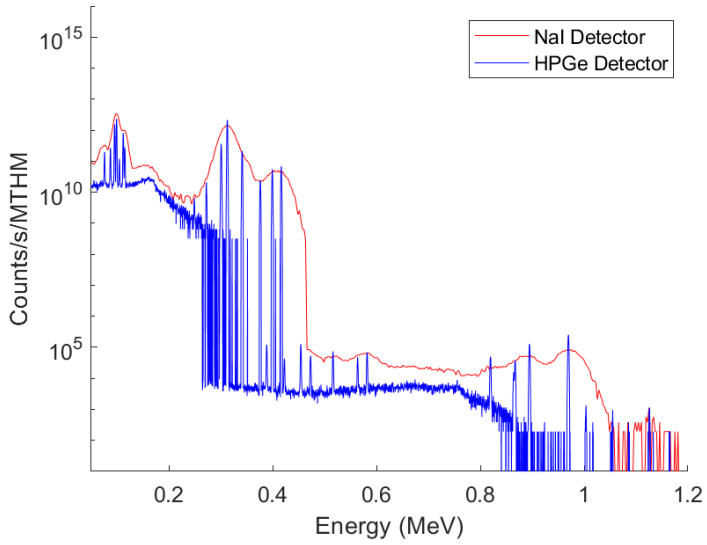

Figure D13: Gamma spectrum for CANDU (0.711% enriched uranium) at 10 days.

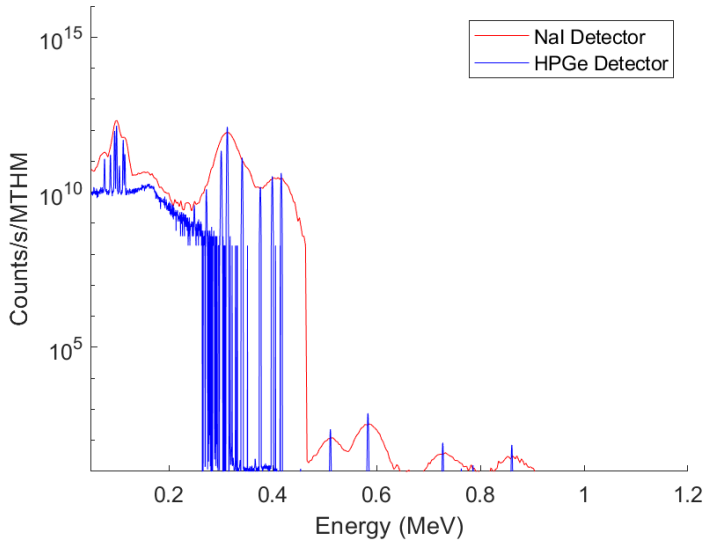

Figure D14: Gamma spectrum for CANDU (0.711% enriched uranium) at 30 days.

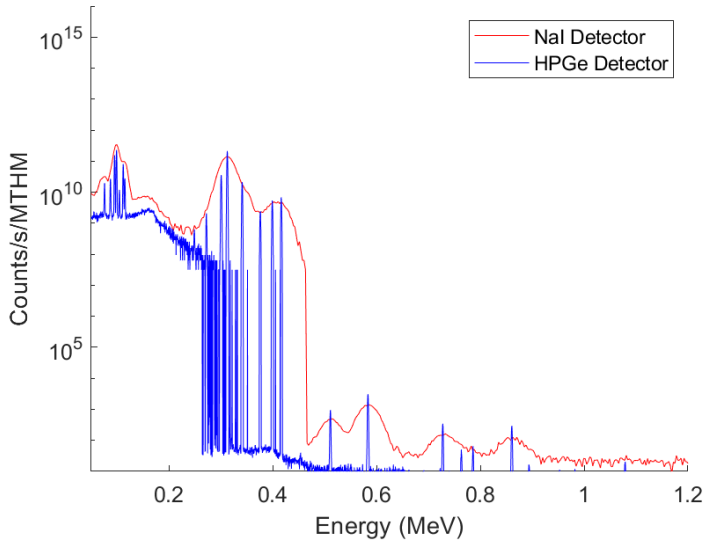

Figure D15: Gamma spectrum for CANDU (0.711% enriched uranium) at 100 days.

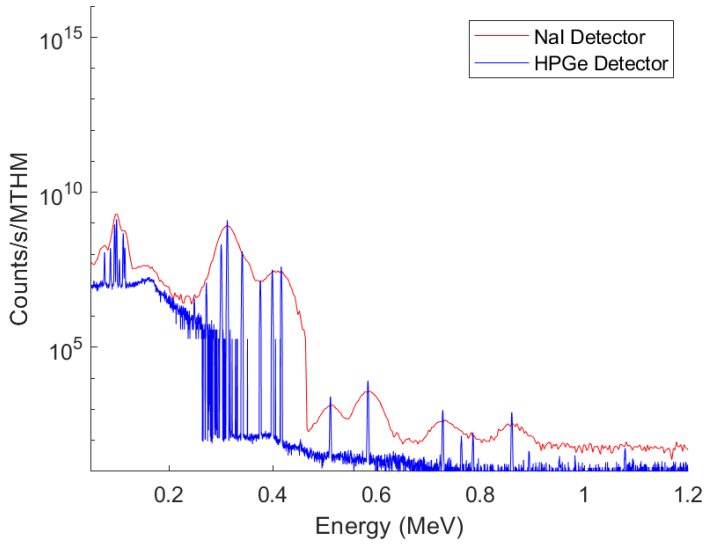

Figure D16: Gamma spectrum for CANDU (0.711% enriched uranium) at 300 days.

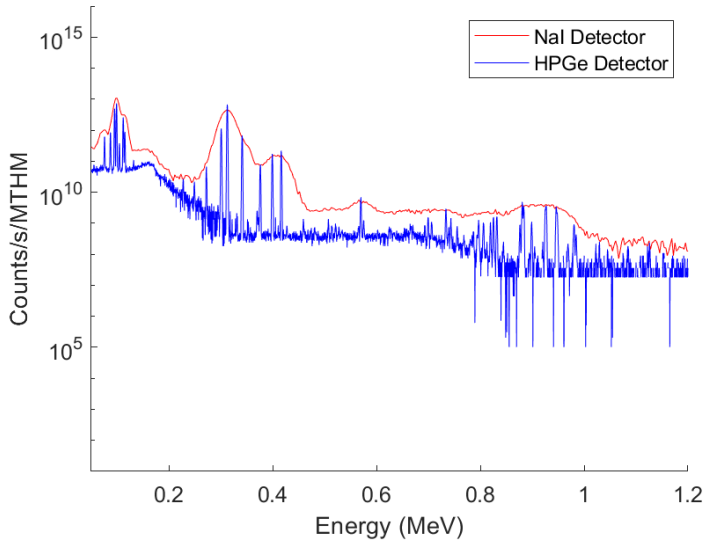

Figure D17: Gamma spectrum for CANDU (19.7% enriched uranium) at 0 days.

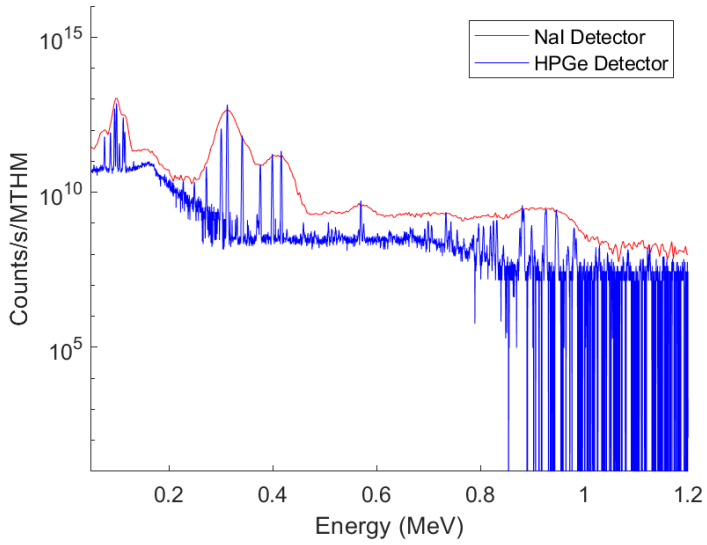

Figure D18: Gamma spectrum for CANDU (19.7% enriched uranium) at 0.1 days.

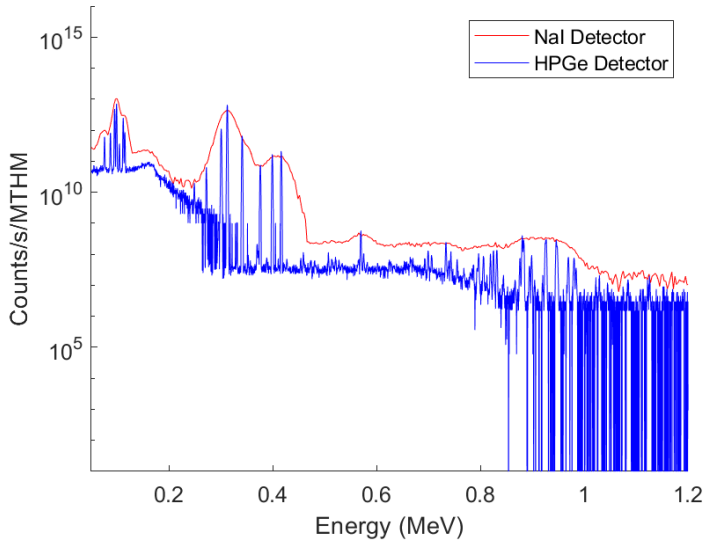

Figure D19: Gamma spectrum for CANDU (19.7% enriched uranium) at 1 day.

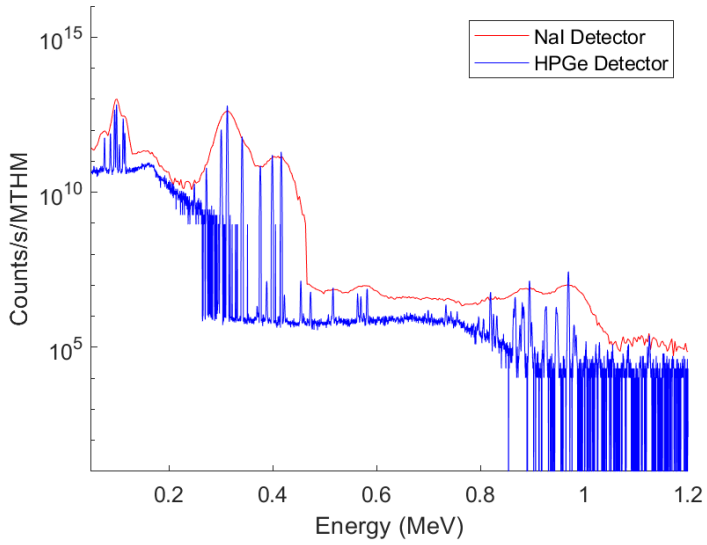

Figure D20: Gamma spectrum for CANDU (19.7% enriched uranium) at 3 days.

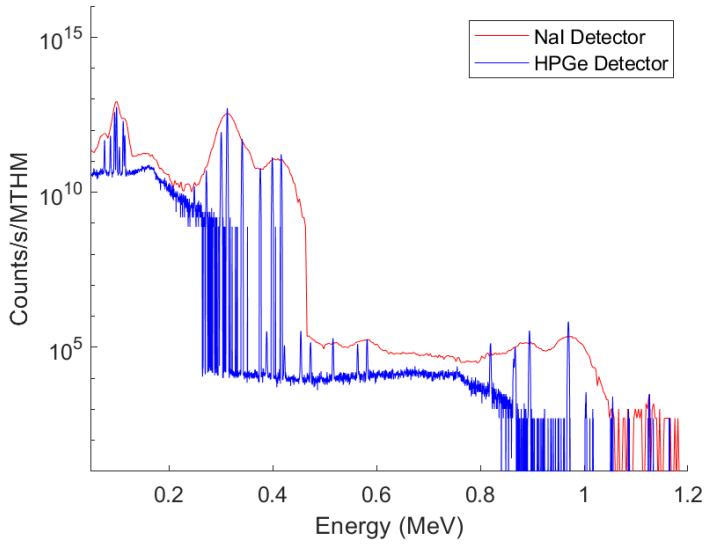

Figure D21: Gamma spectrum for CANDU (19.7% enriched uranium) at 10 days.

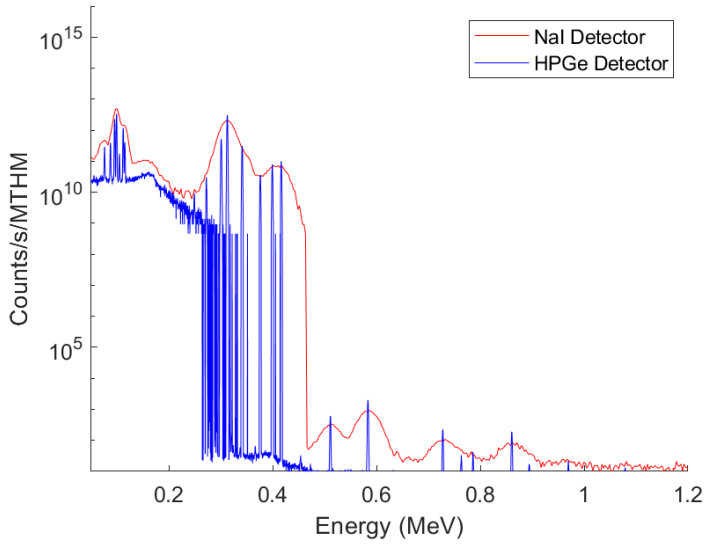

Figure D22: Gamma spectrum for CANDU (19.7% enriched uranium) at 30 days.

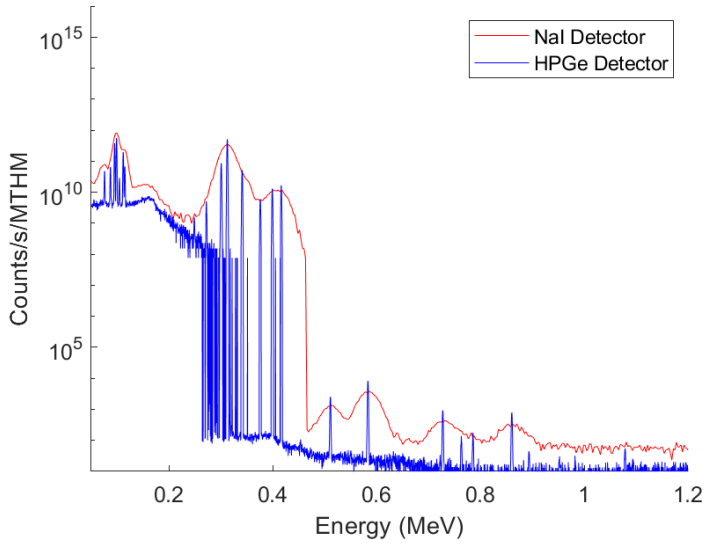

Figure D23: Gamma spectrum for CANDU (19.7% enriched uranium) at 100 days.

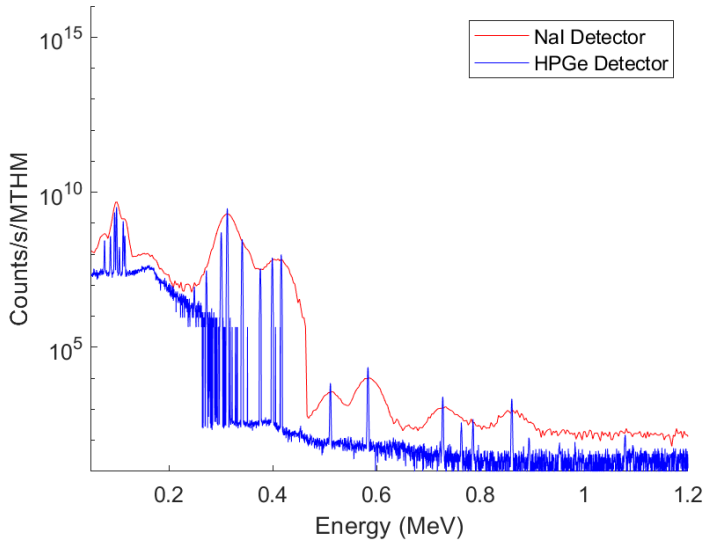

Figure D24: Gamma spectrum for CANDU (19.7% enriched uranium) at 300 days.

APPENDIX E

Gamma spectra for separated protactinium mixture for SCALE Triton simulations.

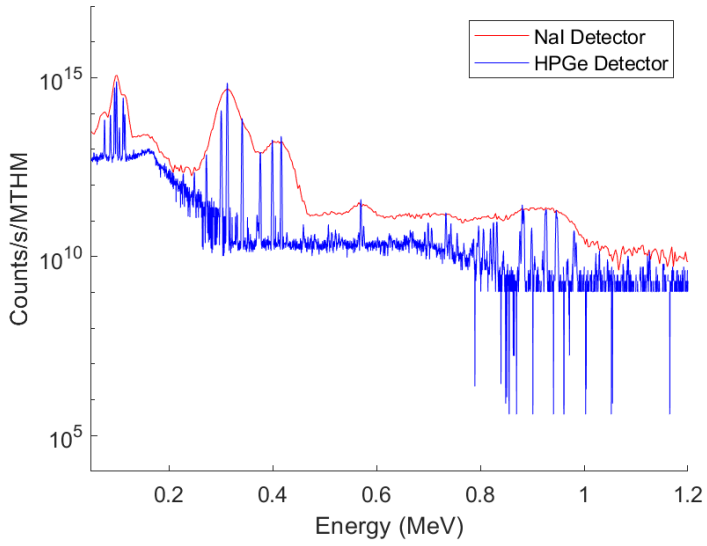

Figure E1: Gamma spectrum for MSR at 2 days.

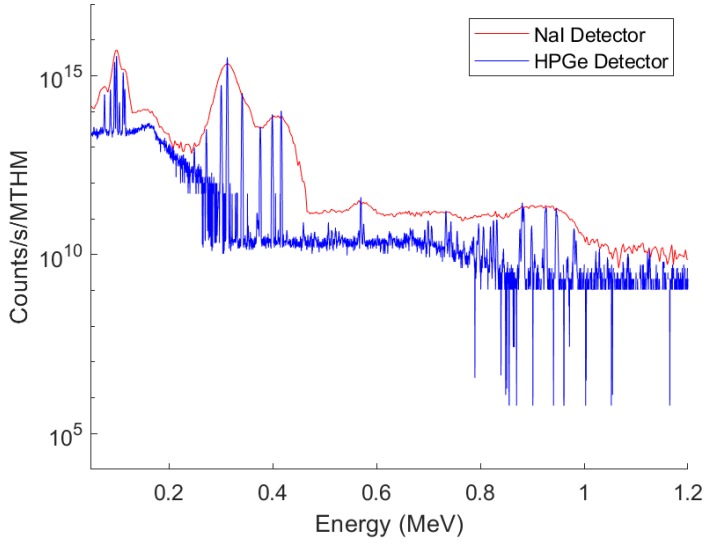

Figure E2: Gamma spectrum for MSR at 10 days.

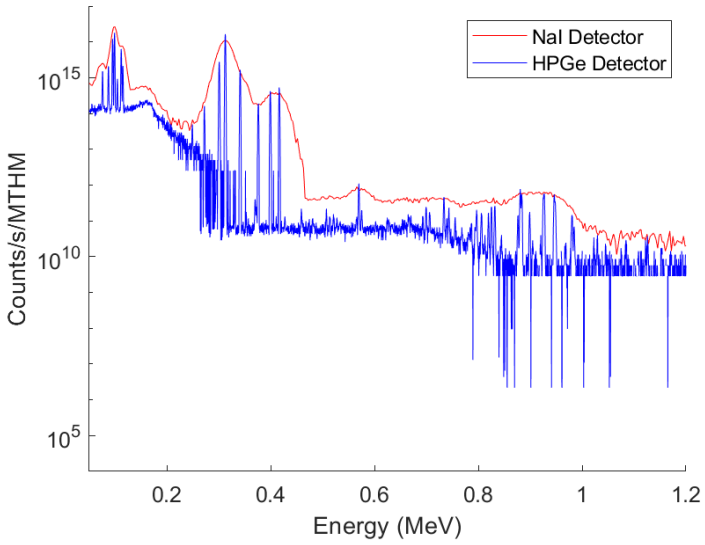

Figure E3: Gamma spectrum for MSR at 30 days.

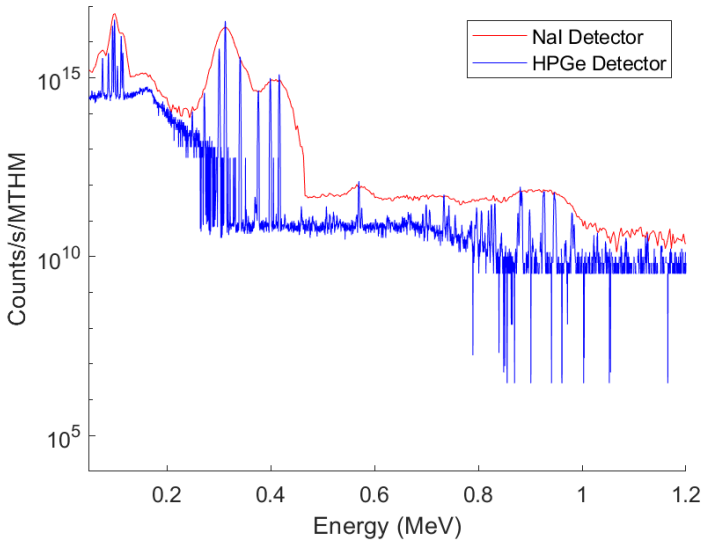

Figure E4: Gamma spectrum for MSR at 100 days.

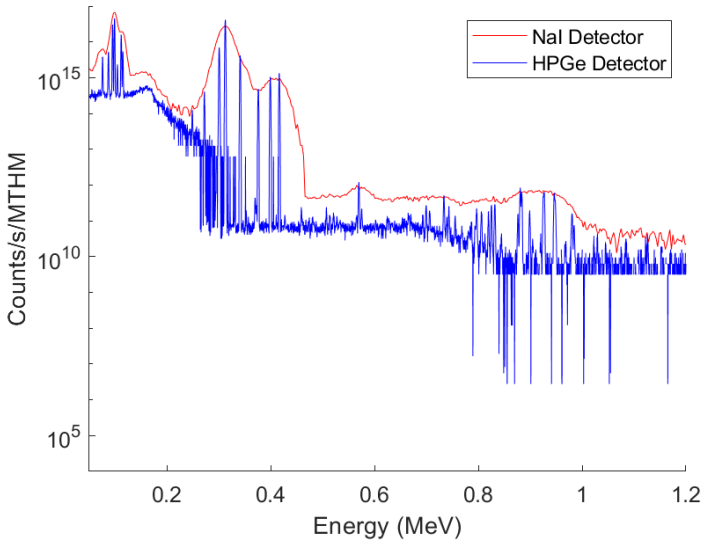

Figure E5: Gamma spectrum for MSR at 300 days.